


ETD Archive

2011

The Parasympathetic Nervous System in Human Heart Failure

Jessica A. French
Cleveland State University

Follow this and additional works at: <https://engagedscholarship.csuohio.edu/etdarchive>

 Part of the [Biology Commons](#)

[How does access to this work benefit you? Let us know!](#)

Recommended Citation

French, Jessica A., "The Parasympathetic Nervous System in Human Heart Failure" (2011). *ETD Archive*. 574.
<https://engagedscholarship.csuohio.edu/etdarchive/574>

This Thesis is brought to you for free and open access by EngagedScholarship@CSU. It has been accepted for inclusion in ETD Archive by an authorized administrator of EngagedScholarship@CSU. For more information, please contact library.es@csuohio.edu.

**THE PARASYMPATHETIC NERVOUS SYSTEM
IN HUMAN HEART FAILURE**

JESSICA A. FRENCH

Bachelor of Science in Biology

Ashland University

December, 2008

Submitted in partial fulfillment of requirements for the degree

MASTER OF SCIENCE IN BIOLOGY

at the

CLEVELAND STATE UNIVERSITY

May, 2011

© Copyright by Jessica A. French 2011

**This thesis has been approved for the
Department of Biological, Geological and Environmental Sciences
and the College of Graduate Studies by**

Thesis Committee Chairperson, Dr. Christine S. Moravec

Department / Date

Dr. Sadashiva S. Karnik

Department / Date

Dr. Crystal M. Weyman

Department / Date

For my mom and dad

*who provided me with infinite opportunities in life,
and strength and support along the way*

ACKNOWLEDGEMENTS

First and foremost, I would like to thank Dr. Christine Moravec, who is not only my major advisor but one of the most extraordinary mentors I have ever had. You have provided me with the tools to earn my Master's degree and to succeed in the future. Thank you for your guidance and support – not only in science but in life. It was an absolute pleasure, every single day, working for you.

I owe a great deal of thanks to my other committee members, Dr. Sadashiva Karnik and Dr. Crystal Weyman. Dr. Weyman, thank you for giving me the opportunity to meet and work with Dr. Moravec and for always making me feel comfortable and confident in pursuing my graduate degree. Dr. Karnik, thank you for taking so much time out of your days to meet with me and guide me through this project. You have provided me with much appreciated advice and knowledge, not only on the muscarinic receptor subtypes, but in science in general. I was extremely lucky to have three amazing committee members, who went above and beyond to help me through the past few years.

To my fellow Moravecians – Dana Frank, Greg Bolwell, Matt Baumann, and Wendy Sweet. Thank you for your continual personal, emotional, and professional support. All of you have made my time in the lab both educational and enjoyable.

A special thank you to Wendy Sweet. I admire you, as a scientist and as a caregiver. Your abilities as an educator have provided me, and so many others, with a better understanding of science and research. Thank You.

Most importantly, I must thank my family and friends. Mom and dad - thank you for giving me all of the opportunities that led me to this point. Thank you for allowing

me to be whoever I wanted to be – a musician, a dancer, an actor, an educated college graduate, and now, a scientist. Mom, Dad, Jenn, Jason, and Jillian – you are my life. Thank you for keeping me grounded throughout all of life’s challenges. To all of my family and to my very closest friends, thank you for being a part of the best memories that I will carry with me forever and for all being the loves of my life. I am the luckiest woman in the world to be surrounded by such remarkable people.

**THE PARASYMPATHETIC NERVOUS SYSTEM
IN HUMAN HEART FAILURE**

JESSICA A. FRENCH

ABSTRACT

Heart failure (HF) affects 5.8 million Americans and is characterized by an inability of the heart to pump blood throughout the body. In a non-diseased state, the sympathetic (SNS) and parasympathetic nervous systems (PNS) innervate the heart to regulate rate and force of contraction. Actions of the PNS on the cardiovascular system are mediated via the vagus nerve, releasing acetylcholine which binds muscarinic receptors on cardiomyocytes. The SNS has been found to be overstimulated in HF, with the role of the PNS in HF unclear. We hypothesized that the PNS is dysregulated in HF, resulting in a change of muscarinic receptor densities. We measured total muscarinic receptor density on non-failing and failing human heart samples, and determined if demonstrated differences were reversed through mechanical unloading with a left ventricular assist device (LVAD). Through radioligand binding assays, we found a significant increase in receptor density in failing human heart samples compared to control (275.8 ± 11.9 versus 194.1 ± 17.3 fmol/mg protein; $p < 0.01$), along with an increase in receptor density in

failing with LVAD support samples(315.8 ± 23.9 versus 194.1 ± 17.3 fmol/mg protein; $p < 0.001$).

We also measured M_1 - M_4 receptor subtypes on a subset of these samples. While the percent of M_1 , M_2 , and M_4 receptor subtypes did not significantly change between non-failing, failing, and failing with LVAD support samples, the percent of M_3 was significantly decreased in failure (8.61 ± 1.65 versus 13.56 ± 2.16 %; $p < 0.05$) and increased back to non-failing percents in the failing + LVAD group (16.65 ± 0.72 versus 8.61 ± 1.65 % in failure; $p < 0.01$).

Muscle function analysis was also performed. Acetylcholine and isoproterenol were used to determine if a change in total muscarinic receptor density in groups related to a change in functional response on fresh trabecular muscles; with and without SNS stimulation. Recovery in contractile parameters without SNS stimulation on ACh-treated muscles, and greater negative inotropic and chronotropic effects on ACh-treated muscles with SNS stimulation provide evidence that total muscarinic receptor density changes elicit different responses on the failing human heart.

TABLE OF CONTENTS

LIST OF TABLES	xi
LIST OF FIGURES	xii
CHAPTER	
I. INTRODUCTION	1
1.1 Human Heart Failure	2
1.2 Left Ventricular Assist Devices (LVADs)	4
1.3 Autonomic Nervous System	7
1.4 Autonomic Nervous System and Heart Failure	8
1.5 Muscarinic Receptors	11
1.6 Research Goal	14
II. METHODS	17
2.1 Human Hearts	17
2.2 Membrane Preparations	19
2.3 Determination of Protein Concentration	20
2.4 Membrane Titer Assay	20
2.5 Measuring Total Muscarinic Receptor Density and Affinity	22
2.6 Measuring Muscarinic Receptor Subtypes	23
2.7 Muscle Function Experiments	26
2.8 Statistical Analysis	31

III. RESULTS	32
3.1 Total Muscarinic Receptor Density and Affinity	32
3.2 Percents of Muscarinic Receptor Subtypes in Non-failing, Failing, and Failing+LVAD Tissue	44
3.3 Muscle Function Analysis	54
IV. DISCUSSION.....	77
4.1 Effect of Total Muscarinic Receptor Density and Affinity in Failure and Upon LVAD Support	77
4.2 Muscarinic Receptor Subtypes in Non-failing, Failing, and Failing+LVAD Human Hearts	81
4.3 Muscle Function	85
4.4 Summary	88
REFERENCES	91

LIST OF TABLES

I.	Characteristics of Patients Used to Measure Total and Subtyped Muscarinic Receptors	33
II.	Characteristics of Patients Used in Muscle Function Studies	57
III.	Baseline Contractile Parameters in NF and F Muscles	59
IV.	Baseline Contractile Parameters in Muscles to be Treated with ACh and Those Muscles Serving as Time Control (TC)	60

LIST OF FIGURES

1.	Non-Failing versus Failing Human Heart	3
2.	Left Ventricular Assist Device	5
3.	β -AR Signaling Pathway	9
4.	Even-Numbered (M_2/M_4) Muscarinic Receptor Signaling Pathway	13
5.	Odd-Numbered ($M_1/M_3/M_5$) Muscarinic Receptor Signaling Pathway	15
6.	Saturation Curve and Lineweaver-Burk Plot	24
7.	Saturation Curve for the Time-Dependent Competition Binding	25
8.	Typical muscle bath set-up	28
9.	Typical muscle contraction with contractile parameters	29
10.	Positive Control Experiment	36
11.	Total Muscarinic Receptor Density	37
12.	Relationship of Muscarinic Receptor Densities to Patient Diagnosis	38
13.	Gender Comparisons Between NF and F Muscarinic Receptor Densities	40
14.	Total Muscarinic Receptor Densities in Different LVAD Types	41
15.	Comparison of duration of LVAD Support to Total Muscarinic Receptor Density	42
16.	Muscarinic Receptor K_d	43
17.	Percents of M_1 Receptor Subtype (Raw Data)	45
18.	Percents of M_2 Receptor Subtype (Raw Data)	46

19.	Percents of M ₃ Receptor Subtype (Raw Data)	47
20.	Percents of M ₄ Receptor Subtype (Raw Data)	48
21.	Percents of M ₁ Receptor Subtype (Normalized Data)	50
22.	Percents of M ₂ Receptor Subtype (Normalized Data)	51
23.	Percents of M ₃ Receptor Subtype (Normalized Data)	52
24.	Percents of M ₄ Receptor Subtype (Normalized Data)	53
25.	Percents of M ₁ and M ₃ Receptor Subtypes	55
26.	Percents of M ₂ and M ₄ Receptor Subtypes	56
27.	Dose-Response to ACh – Resting Tension (RT) Results	61
28.	Dose-Response to ACh – Developed Tension (DT) Results	62
29.	Dose-Response to ACh – Time to Peak Tension (TPT) Results	64
30.	Dose-Response to ACh – Time to Half Relaxation (THR) Results	65
31.	Dose-Response to ACh – Peak Rate of Tension Rise (+dT/dt) Results	66
32.	Dose-Response to ACh – Peak Rate of Tension Fall (-dT/dt) Results	68
33.	Resting Tension (RT) – Isoproterenol (ISO) Response	70
34.	Developed Tension (DT) – Isoproterenol (ISO) Response	71
35.	Time to Peak Tension (TPT) – Isoproterenol (ISO) Response	72
36.	Time to Half Relaxation (THR) – Isoproterenol (ISO) Response	73
37.	Peak Rate of Tension Rise (+dT/dt) – Isoproterenol (ISO) Response	75
38.	Peak Rate of Tension Fall (-dT/dt) – Isoproterenol (ISO) Response	76

CHAPTER I

INTRODUCTION

Heart failure (HF) is a condition affecting approximately 5.8 million Americans every year³⁴. 670,000 new cases are diagnosed annually, and although there are treatment options, 1 in 5 people die within 1 year of diagnosis³⁴. Currently, implantable medical devices and drug therapy are used in the management of HF, however the prevalence of this syndrome continues to be overwhelmingly high. In the heart, rate and force of contraction are regulated by the autonomic nervous system (ANS). Areas of the ANS including the sympathetic nervous system (SNS) are altered in failure, which has led to new drug therapy targets. The counterpart of the SNS, the parasympathetic nervous system (PNS), is not as well understood in HF. With HF being one of the leading causes of mortality, it is important to expand research for more successful treatment options.

1.1 Human Heart Failure

Heart failure (HF) is a disorder characterized by an inability of the heart to pump blood throughout the body⁴⁰. The onset of HF is gradual, and it is the most common diagnosis in patients over the age of 65^{40,18}. This syndrome is heterogeneous, with common symptoms such as breathlessness, fatigue, and fluid retention⁴⁰.

Cardiomyopathy is one diagnosis that leads to HF⁵⁹. There are different types of cardiomyopathy, such as ischemic and dilated cardiomyopathy. As shown in **Figure 1**, these arise when the heart is enlarged and ventricular walls become thin and weakened. Ischemic cardiomyopathy occurs when the heart weakens due to coronary artery disease³⁶. Arteries block with plaque, causing the heart to have difficulty filling and pumping blood to the body³⁶. In dilated cardiomyopathy, the cause is often unknown³⁶. Dilated cardiomyopathy can affect any age group, and can be genetic or caused by alcohol and drug abuse, stress, or a virus³⁶.

Molecularly, HF arises when myocytes undergo remodeling, meaning they change in size, shape, and function⁷. Remodeling is an effect of cardiomyocytes responding to biomechanical stressors stimulating molecular and cellular events that lead to the characteristic failing heart^{7,43}. At first, these events are stimulated to compensate for the failing heart. But after continual stimulation, they progressively exacerbate the disease and worsen prognosis. These events are a complex series of interactions that mediate various responses on the heart, including rate and force of contraction. Examples of important changes seen in HF include alterations in calcium-cycling proteins and autonomic nervous system regulation^{10,13,40}.

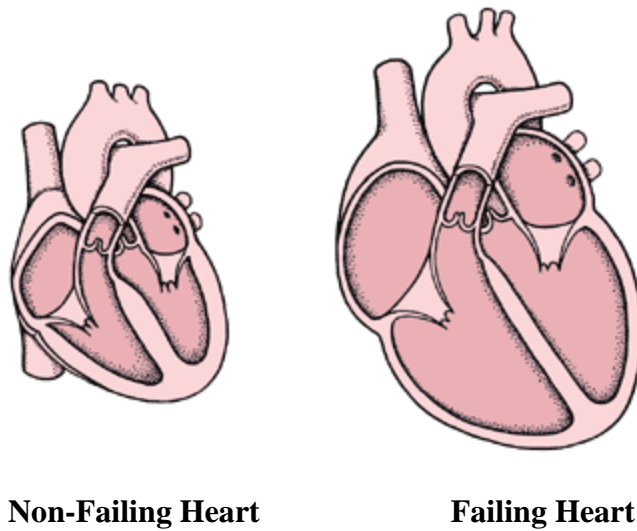


Figure 1. *Non-Failing versus Failing Human Heart.*

Non-failing (NF) human hearts, about the size of a clenched fist, are significantly smaller than severely failing hearts. Notable features of the failing heart include enlarged chambers and thinned ventricular walls. (Figure modified from www.intensivecare.hsnet.nsw.gov.au)

Alterations in Ca^{++} signaling contribute to depressed contractility seen in HF. Because of the complexity of Ca^{++} regulation in healthy hearts, it is difficult to pinpoint exact causes of reduced Ca^{++} transport in failure. One mechanism involves the sarcoplasmic (endoplasmic) reticulum Ca^{++} ATPase protein SERCA. Studies have shown a reduction in SERCA signaling in HF and improved contractility upon increased expression^{23,24}. The protein that interacts with SERCA to inhibit reuptake of Ca^{++} , phospholamban (PLB), is also a target of investigation. Research supports that decreased levels of PLB play a role in decreased Ca^{++} . Along with finding decreased levels of SERCA and PLB, investigators have shown decreased expression of L-type Ca^{++} channels and ryanodine receptors (RYRs), and increased expression of Na^{+} - Ca^{++} exchanger (NCX)²³.

The complexity of HF makes the condition difficult to treat. Heart transplantation is the most effective form of treatment, yet only about 2,300 patients each year are able to receive a transplant²¹. Drug therapy, surgery, and device therapy are currently the mainstay in managing HF.

1.2 Left Ventricular Assist Devices (LVADs)

Left ventricular assist devices, or LVADs, are surgically-implanted pumps that run via battery. They take over pumping ability in severely failing hearts when heart transplantation is not presently available³¹. During LVAD support, hearts are hemodynamically unloaded so they can continue to beat without having to perform work. As shown in **Figure 2**, LVADs are implanted from the apex of the left ventricle to the

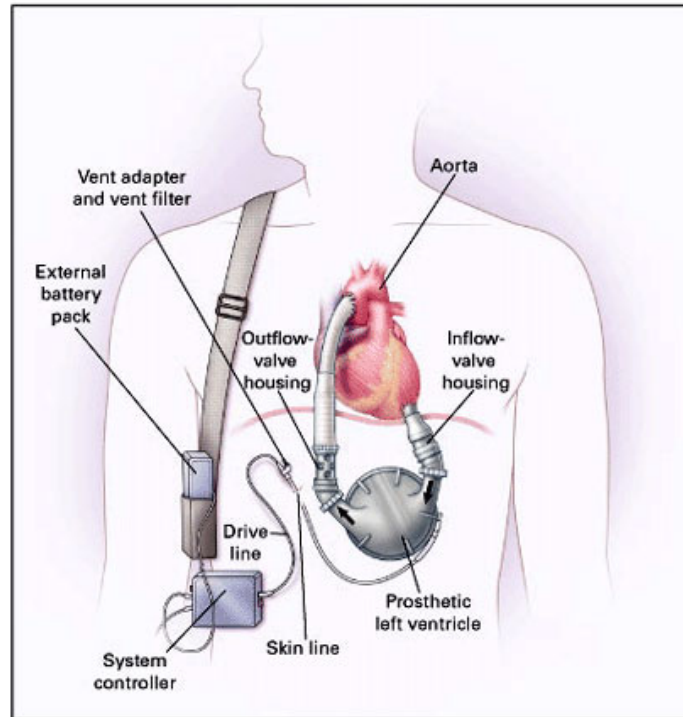


Figure 2. Left Ventricular Assist Device. Although differing models of LVADs are available, typical devices are implanted from the apex of the left ventricle to the ascending aorta, with a pump lying in the abdomen or thoracic cavity. These devices take the workload off of the left ventricles by allowing blood to flow through the left ventricle, while the device pumps the blood out to the aorta. (Figure from www.heartfailure.org)

ascending aorta. Blood is pumped from the lungs to the left atrium and into the left ventricle. Blood is pulled from the left ventricle and into the device. The device pumps blood into the aorta to be sent systemically through the body. The pump's battery and control system are kept outside the body, and are connected through a drive line to the pump inside the body.

LVADs were first used as a bridge-to-transplant therapy for patients on the cardiac transplantation list. However, research in the past decade has shown LVADs to increase survival rates and prognosis, leading to implantation of these devices as destination therapy^{20,48}.

Rose et al found that patients with LVAD support survived a median 408 days while patients without a device survived a median 108 days⁴⁸. Physical ability exams and quality of life questionnaires were also examined from the same patient population, resulting in significantly higher physical function and qualities of life in patients with LVAD support.

At the myocyte level, there is evidence that LVADs reverse remodeling of the failing heart. In failing hearts treated with LVADs, contractile function of myocytes recovered²⁰. Contractile functions restored included the magnitude of shortening, and developed tension and relaxation rates^{20,42}. LVAD support also was found to improve neurohormonal systems, calcium handling, cytoskeletal protein abundance, and metabolic signaling^{12,14,20,28,53}. Beta-adrenergic receptor signaling, a component of the ANS, was also restored upon LVAD support⁴².

1.3 Autonomic Nervous System

The ANS regulates functions of the body, including airflow, body temperature, digestion, blood pressure, and heart rate⁴⁹. It is often referred to as a ‘self-governing’ system and controls processes that are responsible for maintaining homeostasis⁴⁹. There are two major divisions of the ANS: the sympathetic (SNS) and parasympathetic (PNS) nervous systems. These two systems innervate the same target organs, and either cooperate or contrast with one another to produce different effects on the body⁴⁹. The SNS and PNS are not opposites; rather, they form a web of complex interactions responsible for maintaining proper balance between the two systems⁴⁴. The SNS and PNS can, depending on the target organ, be either stimulatory or inhibitory and act simultaneously to produce an effect⁴⁹.

The SNS is often referred to as the ‘fight or flight’ division of the ANS. It adapts the body for more physically active situations, and is usually employed in states of arousal, anger, danger, fear, etc⁴⁹. In the heart, stimulation of the SNS causes an increase in heart rate and force of contraction.

The PNS is often referred to as the ‘rest or digest’ division of the ANS. It is used predominantly in non-physically active situations such as in the process of digestion. In the heart, stimulation of the PNS causes a decrease in heart rate and force of contraction and is of stronger influence than the SNS at rest. PNS signals to the heart travel through the vagus nerve, one of the cranial nerves. The brain receives signals from sensory receptors about conditions of the heart such as heart rate before signals are sent to carry out necessary responses. In the PNS, long preganglionic nerve fibers carry the signal

from the brain and synapse with short postganglionic nerves. At the synapse, acetylcholine is released and binds to nicotinic receptors on postganglionic fibers. The signal travels through these fibers and reaches the target organ. Here, acetylcholine is released again, this time binding to muscarinic receptors on cardiomyocytes⁴⁹.

1.4 Autonomic Nervous System and Heart Failure

An imbalance of the ANS is a defined characteristic in the progression of HF¹. Because of this, it is important to be able to evaluate autonomic activity in cardiovascular disease. Research concludes that increase in SNS activity and decrease in PNS activity are related to an increased risk of death in cardiovascular disease²⁹. However, it is difficult to quantify ANS activity because of its complexity²⁹. Therefore, exploring various markers that reflect autonomic activity remains a vital area of research.

The SNS increases heart rate and force of contraction in a non-diseased state. It is activated when norepinephrine (NE) binds to beta-adrenergic receptors (β -AR) on cardiomyocyte plasma membranes (signaling pathway depicted in **Figure 3**). These β -ARs interact with heterotrimeric G_s proteins that stimulate adenylyl cyclase. This effector molecule dissociates ATP into cyclic-AMP to bind protein kinase A (PKA). PKA phosphorylates L-type Ca^{++} channels, RYRs, PLB, and troponin I, which causes an increase of Ca^{++} movement. Increase in Ca^{++} ultimately causes a positive inotropic and chronotropic effect on the heart.

In HF, the SNS is overactivated. This system first acts to compensate for declining cardiac function, yet long-term activation decompensates cardiac function⁵⁵. A notable

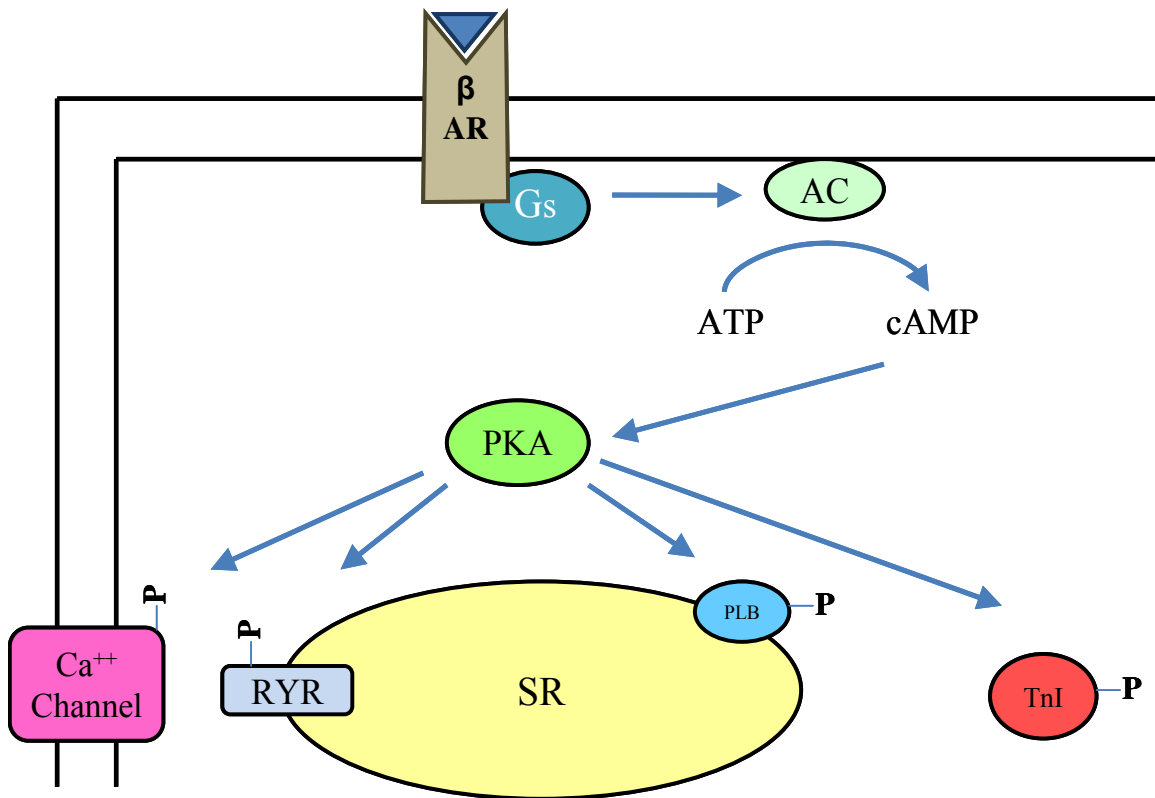


Figure 3. β -AR Signaling Pathway. Agonists, such as norepinephrine bind to β -ARs on cardiac myocytes which stimulates Gs proteins to active adenylyl cyclase (AC). Through downstream signaling, proteins that increase Ca^{++} movement within the cell are activated by phosphorylation. An increase in Ca^{++} movement results in a positive inotropic and chronotropic effect.

and well-studied feature of the SNS in HF is alterations in β -AR density. It has been found that β -AR density is significantly downregulated in the failing heart^{4,13,55}. Specifically, the ratio of β -AR subtypes, β_1 and β_2 , drop from approximately 75:25 in a non-diseased state to 60:40 during failure⁴. β_1 -AR population decreases while β_2 does not significantly change⁴. β -AR downregulation is the result of high concentrations of NE leading to desensitization of the receptor. What has been developed with the 20⁺ years of research on β -ARs are drug therapies targeting and blocking these SNS receptors from activating signaling pathways. These drugs, commonly called β -blockers, are now universally used to decrease sympathetic overactivation in the failing heart. In studying LVAD support and the SNS, β -AR density has been shown to be restored through LVAD support with densities closely mimicking non-failing results⁴².

The role of the PNS in HF is not as clear. It is established that autonomic dysfunction in HF is related to overactivation of the SNS and attenuation of the PNS. To examine PNS control, vagal nerve studies have been an area of recent research. Stimulation of the vagus nerve has improved cardiac function and increased survival in various models of HF^{33,51,54,61}. This occurs primarily because acetylcholine released from the vagus interacts with cholinergic receptors on cardiomyocytes and inflammatory cells⁵⁴. PNS regulation of heart rate is increased, along with inhibiting release of inflammatory cytokines such as tumor necrosis factor (TNF) and interleukin-1 (IL-1)⁵⁴. With these changes upon vagal stimulation, autonomic balance improves and inflammatory responses are suppressed⁶¹. Vagal nerve stimulation is shown to be of potential therapeutic benefit and is one way of targeting the PNS in HF.

Because SNS activity was studied using the target membrane receptor on cardiomyocytes, another way to examine PNS activity is to study the target receptor of the PNS: muscarinic receptors. Up to this point, attempts to study the PNS in HF this way have led to conflicting results, thereby no definitive conclusions have been drawn^{1,3,19,32,56}.

1.5 Muscarinic Receptors

Muscarinic receptors belong to the family of receptors known as g-protein coupled receptors (GPCRs). GPCRs are one of the most abundant and diverse of protein families, and the most common type of cardiac receptor^{27,47}. There are an estimated six major classes of GPCRs, which are thought to be of early evolutionary origin due to their presence in bacteria and yeast²⁷. The ANS utilizes adrenergic and muscarinic cholinergic receptors to maintain homeostasis in the heart and cardiovascular system⁴⁷. Muscarinic receptors are expressed in a variety of cells and are further broken down into five specific subtypes^{5,16}. These subtypes are named M₁-M₅, based on the order of their discovery¹⁶. Muscarinic receptors are composed of seven transmembrane alpha helices, with an extracellular N-terminus and intracellular C-terminus²⁷. These seven hydrophobic transmembrane domains are connected by three extracellular and three intracellular hydrophilic loops¹⁶. M₁-M₅ share 90% of their amino acid sequences within their hydrophobic domains and differ the greatest in their loop and tail regions¹⁶. In the heart, M₂ is thought to be the most predominant, and at one time, was thought to be the only

subtype present on cardiomyocytes^{5,8,45}. More recent studies, however, have suggested multiple subtypes existing in mammalian heart tissue^{52,58}.

Muscarinic receptor subtypes differ in signaling pathways. All GPCRs rely on an extracellular stimulus to activate intracellular signals via interaction of heterotrimeric G proteins with the receptors' intracellular loops²⁷. In basic signal transduction, a ligand binds to its appropriate receptor to stimulate a conformational change of the receptor. This change in conformation leads to activation of an associated heterotrimeric G protein, allowing for the G protein's α subunit to dissociate from its β and γ subunits. The G protein subunits activate and amplify signals within the cell by altering activity of an effector molecule. The activities of the effectors control production of second messenger molecules leading to a variety of downstream signaling pathway activation^{16,27,47}.

Although all muscarinic receptors use this basic signal transduction mechanism, the subtypes differ in G proteins, effectors, and second messengers, leading to different cellular responses. The even-numbered muscarinic receptor subtypes, M_2 and M_4 , couple to a G_i protein, while M_1 , M_3 , and M_5 interact with a G_q protein. For all five subtypes, initial conformational change occurs when acetylcholine binds to the receptor. Illustrated in **Figure 4**, M_2 and M_4 , upon activation of G_i , inhibit adenylyl cyclase (AC) activity, leading to a reduction in intracellular levels of cAMP¹⁶. This inhibits cyclic AMP-dependent kinases (PKA) from phosphorylating proteins such as L-type Ca^{++} channel, RYRs, PLB, and troponin I, causing a decrease in movement of Ca^{++} . This pathway antagonizes the SNS signaling pathway and is active after stimulation of the SNS. Even-numbered muscarinic receptors also directly open K^+ channels on the plasma membrane,

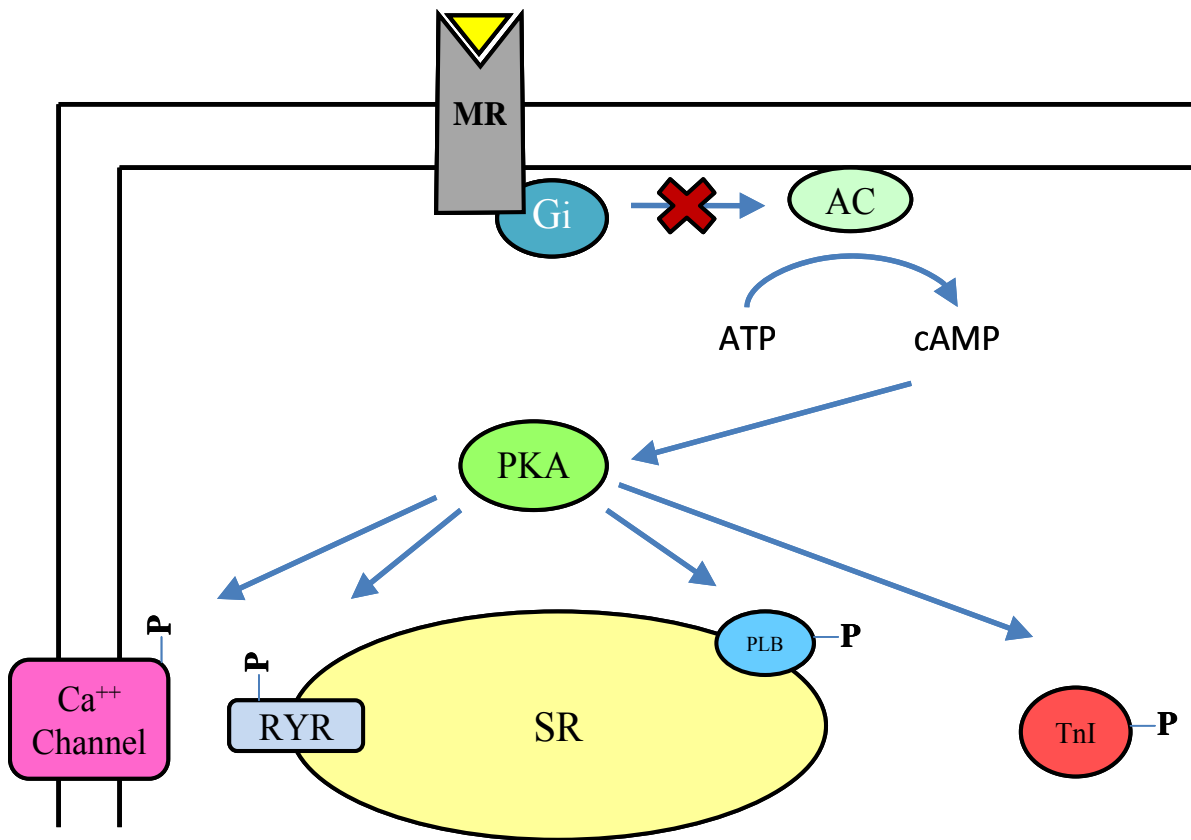


Figure 4. Even-Numbered (M_2/M_4) Muscarinic Receptor Signaling Pathway. Agonists, such as acetylcholine (ACh), bind to muscarinic receptors on cardiac myocytes which activate Gi proteins. Gi proteins antagonize the β -AR signaling pathway by inhibiting AC from increasing intracellular cAMP levels. This results in a decrease in Ca^{++} movement within the cell which produces a negative inotropic and chronotropic effect on the heart.

turning off the electrical signals caused by depolarization, reducing contractility, however evidence in ventricular tissue is lacking²⁵. M₁, M₃, and M₅, upon activation of G_q, activate phospholipase C (PLC) (signaling pathway depicted in **Figure 5**). PLC hydrolyzes phosphatidylinositol 4,5-bisphosphate (PIP₂) to inositol 1,4,5-trisphosphate (IP₃) and diacylglycerol (DAG)^{5,16}. DAG stimulates protein kinase C (PKC) while IP₃ releases Ca⁺⁺ from the SR, leading to an increase in heart rate and force of contraction²⁵. Because the M₂ receptor subtype is thought to exert greater influence than the other subtypes on cardiomyocytes, the predominant effect of muscarinic stimulation to the heart is inhibitory.

1.6 Research Goal

The goal of this project is to study the role of the PNS in human HF. The hypothesis that the PNS is dysregulated in human HF will be tested using muscarinic receptor density as a measurable variant of PNS activity. Total muscarinic receptor densities will be measured using a modified radioligand binding assay protocol, while muscarinic subtypes will be measured using a time-dependent competition binding assay. With these established techniques, muscarinic receptor densities in non-failing and failing human heart samples will be analyzed. Muscarinic receptor densities in failing tissue samples from patients who had LVAD support will also be studied. This population will allow us to explore the restoring capabilities of LVADs on the PNS. Once densities in nonfailing, failing, and failing + LVAD support heart tissue samples are measured, muscle function analyses will be performed. Muscle function experiments will provide insight on the

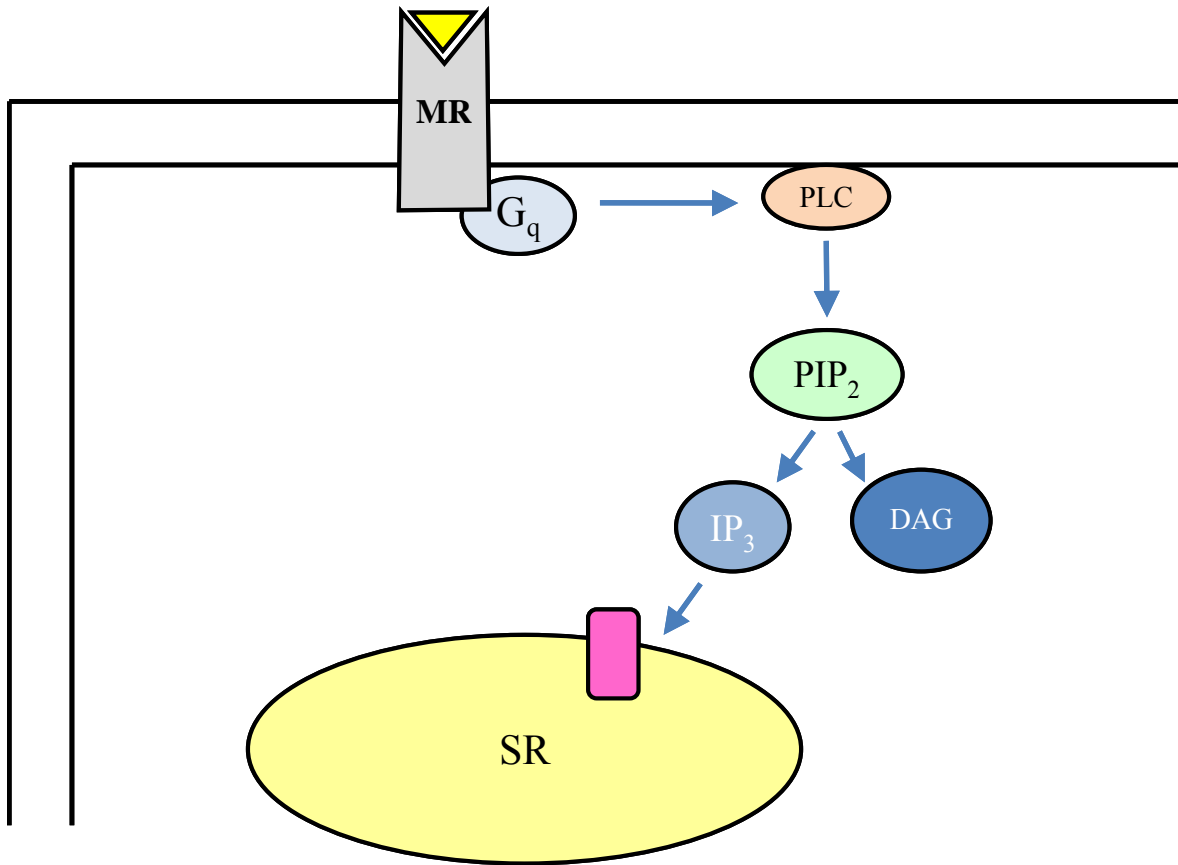


Figure 5. Odd-Numbered ($M_1/M_3/M_5$) Muscarinic Receptor Signaling Pathway. Agonists, such as acetylcholine, bind to odd-numbered muscarinic receptors on cardiac myocytes which stimulate Gq proteins. Gq proteins activate phospholipase C (PLC) which hydrolyzes PIP₂ into IP₃ and DAG. DAG activates a downstream pathway by PKC while IP₃ directly activates Ca⁺⁺-channels on the SR, leading to an increase in Ca⁺⁺ release. This increase in Ca⁺⁺ results in a positive inotropic and chronotropic effect. (Abbreviations: PIP₂ = phosphatidylinositol 4,5-bisphosphate; IP₃ = inositol 1,4,5-trisphosphate; DAG = diacylglycerol; PKC = protein kinase C; SR = sarcoplasmic reticulum)

inotropic response of fresh trabecular muscle upon acetylcholine and isoproterenol stimulation. Results from these experiments will be used to compare contractility changes to receptor density changes in each population. Conclusions found through the data analysis may provide for a novel approach in tackling human heart failure, leading to better and more effective treatment options.

CHAPTER II

METHODS

2.1 Human Hearts

Human hearts were obtained from a patient population only after IRB approval and patient consent. Left ventricular (LV) tissue was obtained from patients with non-failing hearts, failing hearts, and failing hearts which had been supported by an LVAD prior to transplant. Non-failing and failing samples were used to compare the effects of heart failure on muscarinic receptor density. In anticipation of finding differences, a second failing group was studied to explore the recovery of muscarinic receptors by mechanical unloading in patients with an LVAD (failing + LVAD). Non-failing hearts were obtained from unmatched organ donors whose hearts were unsuitable for transplantation. Failing and failing + LVAD groups were the explanted hearts of cardiac transplant recipients at Cleveland Clinic. Inclusion criteria for donor sample selection were males and females, between 40-65 years of age. Since left ventricular ejection fractions above 50% demonstrate normal cardiac function, only donor hearts with ejection fractions $\geq 50\%$

were included. Inclusion criteria for failing and failing + LVAD samples were males and females, between 40-65 years of age, with an ejection fraction <35%. Exclusion criteria included pacemakers because of the unknown effect pacing may have on autonomic nervous system regulation. Samples were also excluded if patients were on drugs with potential muscarinic interactions. These included sotalol, amiodarone (for non-failing and failing samples only), disopyramide, quinidine, and atropine. These drugs were excluded based on previously reported drug/receptor interactions^{9,11,38,39,41}. Right atrial tissue was also obtained from heart failure patients undergoing cardiac transplantation and a piece of de-identified brain tissue was acquired from the Department of Pathology at CC. Both served as positive controls.

For muscle function analyses, fresh trabecular muscles were taken from non-failing and failing patients immediately following acquirement of tissue from operating rooms. Non-failing left ventricular tissue came from patients with hypertrophic cardiomyopathy (HOCM) and failing left ventricular tissue came from explanted hearts of cardiac transplant recipients at Cleveland Clinic. Non-failing tissue included both males and females, aged between 41-74 years, and with ejection fractions >50%. Failing tissue included both males and females, between 46-68 years of age, with ejection fractions below 35%.

2.2 Membrane Preparation

Frozen human heart samples were broken into pieces weighing 2.0-2.2 g and placed into Buffer A [composition: 10mM (4-(2-hydroxyethyl)-1-Piperazineethanesulfonic acid (HEPES), 5mM Ethylene glycol tetraacetic acid (EGTA), 12.5mM Magnesium Chloride ($MgCl_2$), 250mM Sucrose, 10mg/mL Leupeptin, 20 μ g/mL Phenylmethanesulfonylfluoride (PMSF), 20 μ g/mL Bacitracin, 20 μ g/mL Benzamidine]. Samples were homogenized in 3 second bursts with 5 second rests on ice until no chunks of tissue remained. Homogenates were centrifuged at 300 x g for 5 minutes at 4°C to pellet out heavier organelles such as nuclei and mitochondria. Supernatants (containing lighter cytosolic fragments such as actin/myosin filaments and membrane fragments) were incubated in 0.5M KCl solution for 15 minutes at 4°C to destroy the myofilaments in the supernatant. Suspensions were centrifuged at 40,000 x g for 15 minutes at 4°C to pellet the membrane fraction. The supernatant was discarded and pellets were added to buffer B, a non-sucrose containing buffer [composition: 20mM HEPES, 5mM EGTA, 12.5mM $MgCl_2$, 100mM NaCl; and 20 μ g/mL each of Leupeptin, PMSF, Bacitracin, and Benzamidine)]. In buffer B, pellets were Dounce homogenized (10 times slowly with a loose plunger followed by 10 times slowly with a tight plunger) to refine the membrane fraction. Once each sample was homogenized, preparations were centrifuged to re-pellet membrane preparations (40,000 x g for 15 minutes at 4°C). Pellets underwent a second series of homogenization to further refine the membranes. Preparations were centrifuged at 40,000 x g for 15 minutes at 4°C. Final pellets were added to buffer B + 10% glycerol

to help preserve the membranes upon storage. Pellets were resuspended using a motorized homogenizer until they were fully suspended. Aliquots were stored at -80°C.

2.3 Determination of Protein Concentration

Lowry protein assays were performed on membrane preparations to determine total protein concentrations. Standards containing known concentrations (0.0, 0.5, 1.0, 2.0, 3.0, 4.0 mg/mL) of bovine serum albumin (BSA) were added to a 96 well plate, in triplicate. 1:2 dilutions of membrane preparations were also added in triplicate to the 96 well plates. Reagent A, a solution that recognizes peptide bonds and binds to all protein, was added to each standard and sample. Reagent B, a solution that recognizes reagent A and, upon binding, produces a color change, was then added to each well. The standards and samples were incubated for 15 minutes at room temperature. The absorbance was read at 750nm. The known concentrations of BSA were used to generate a standard concentration curve from each standard's measured absorbance and this was then used to determine the unknown sample concentrations.

2.4 Membrane Titer Assay

A radioligand binding assay was used to measure total muscarinic receptor density and affinity. Before beginning these experiments, the amount of membrane necessary to attain 10% specific binding was determined using a membrane titer assay.

In a membrane titer assay, a non-selective radiolabeled antagonist (³H-Quinuclidinyl benzilate) is added to membrane to determine total binding to muscarinic receptors. Non-

specific binding is determined by adding ^3H -QNB in the presence of a second non-selective and non-labeled muscarinic receptor antagonist (atropine). Atropine is added in a high concentration in order to ensure atropine binding to the muscarinic receptor, such that any radioactivity remaining is due to ^3H -QNB binding to something other than receptor. By subtracting non-specific binding from total binding, specific binding can then be determined. ^3H -QNB is also measured in the absence of membrane to ascertain total counts of radioactivity. Final calculations are performed to determine the amount of membrane needed for specific binding to equal 10% of total counts of radioactivity. Details for this assay are as listed below.

All steps prior to incubation were performed on ice. Six 12x75mm polypropylene tubes were used for each heart sample: three to measure total binding in triplicate and three to measure non-specific binding, also in triplicate. A buffer containing 20mM HEPES, 15mM EGTA, 1.25mM MgCl_2 (HEM) and 0.1% BSA was added to all total binding and non-specific binding tubes and was used to prepare ^3H -QNB, atropine, and membrane.

For this assay a theoretical K_d taken from the literature was used⁵⁸. 250pM of ^3H -QNB was added to all total binding, non-specific binding, and total count tubes. Atropine (non-selective, non-labeled) was added to the non-specific binding tubes to achieve a 1 μM antagonist concentration.

Membrane preparations were added last. Frozen aliquots of tissue samples were thawed on ice and diluted to 25 μg protein per tube. Preparations were added to total and non-specific binding tubes.

Tubes (with a final volume of 250 μ L) were mixed on a Vortex mixer and placed in a shaking water bath for 1 hour at 37°C. After incubation, preparations were harvested onto GF/C filter paper, and washed five times with cold HEM. Filters were cut out and placed in 7mL scintillation vials and set in a 42°C oven to dry. Once dried, 5mL of Cytoscint ES scintillation fluid was added to each vial. Vials were capped, mixed, and then wiped with a dryer sheet (to avoid artificially high values due to static discharge). Vials were read in a scintillation counter for two minutes each.

2.5 Measuring Total Muscarinic Receptor Density and Affinity

A radioligand binding assay was used to measure total muscarinic receptor density and K_d. In this assay, multiple doses of ³H-QNB were added to samples to generate a saturation curve and Lineweaver-Burk plot.

Forty-eight 12x75mm polypropylene tubes were used per heart. For each heart, three tubes were used to measure total binding and three were used to measure non-specific binding (run in triplicate) at each dose of radioactivity. Eight doses of radioactivity were utilized in this assay.

Eight differing doses of ³H-QNB were made. The highest dose (1500pM) of radioactivity was prepared and the seven other doses were serial diluted from the highest dose to achieve final concentrations [concentrations in pM: 11, 27, 68, 135, 270, 540, 900, 1500]. Buffer and atropine were added as described in Section 2.4.

Membrane preparations were added last. Frozen aliquots of tissue samples were thawed on ice and diluted to amounts determined by the membrane titer assay.

Tubes were mixed and placed in a shaking water bath for 1 hour at 37°C. After 1 hour, preparations were harvested onto GF/C filter paper, dried, and read as described in Section 2.4.

Results generated a saturation curve measuring concentration of radioactivity to amount of binding. A Lineweaver-Burk plot was created by plotting binding (pmol/mg) to the ratio of bound vs. free radioactivity. The x-intercept of this plot was equivalent to the Bmax (density) of the sample and the slope equals the Kd. An example of a saturation curve and Lineweaver-Burk plot is depicted in **Figure 6**.

2.6 Measuring Muscarinic Receptor Subtypes

Muscarinic receptor subtypes were measured using a time-equilibrium binding assay. In this assay, one concentration of radioactivity was used and changes in binding were measured over a two hour time course in the presence of the selective non-labeled antagonist for each subtype. Saturation curves were generated to determine the fraction of each subtype. An example is shown in **Figure 7**.

One hundred and eighty 12x75mm polypropylene tubes were used per heart. Thirty tubes were used for each condition (total binding, nonspecific binding, antagonist binding for M₁, M₂, M₃, and M₄). Buffer and atropine was added as described in Section 2.4. After preliminary studies and a literature search, K_i's were determined for the project. To measure subtypes, non-labeled subtype-selective antagonists were used [in 1mM: M₁ – Pirenzepine, M₂ – Methoctramine, M₃ – p-Fluoro-hexahydrosila-difenidol (pf-HHSiD), M₄ – Tropicamide]. No current subtype selective antagonist is available for M₅ and this

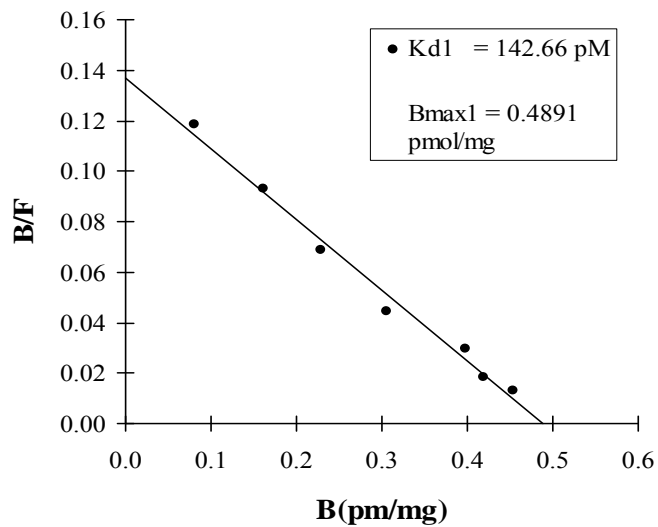
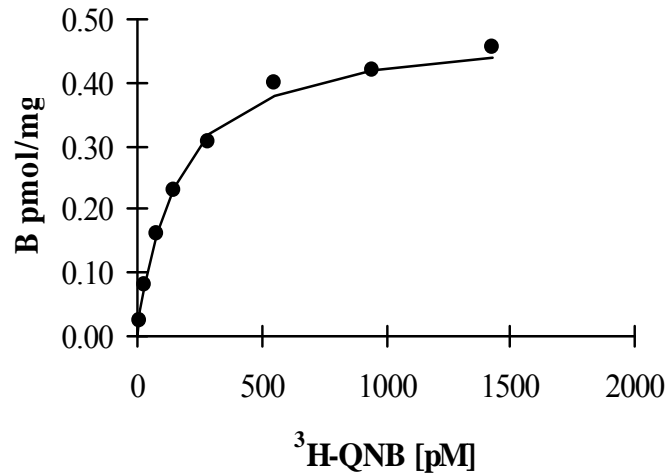


Figure 6. Saturation Curve (Top) and Lineweaver-Burk Plot (Bottom).

Radioligand binding assays generate a saturation curve and Lineweaver-Burk plot to determine density and K_d of samples. The Lineweaver-Burk plot is a linear interpretation where specific binding is plotted against the ratio of bound to free radioactivity. The x-intercept of a Lineweaver-Burk plot is the B_{max} , or density of the receptor of interest. The K_d is interpreted by the slope of the line. (Abbreviations: B = Specific Binding, B/F = Specific Binding divided by the Concentration of Free Radioligand)

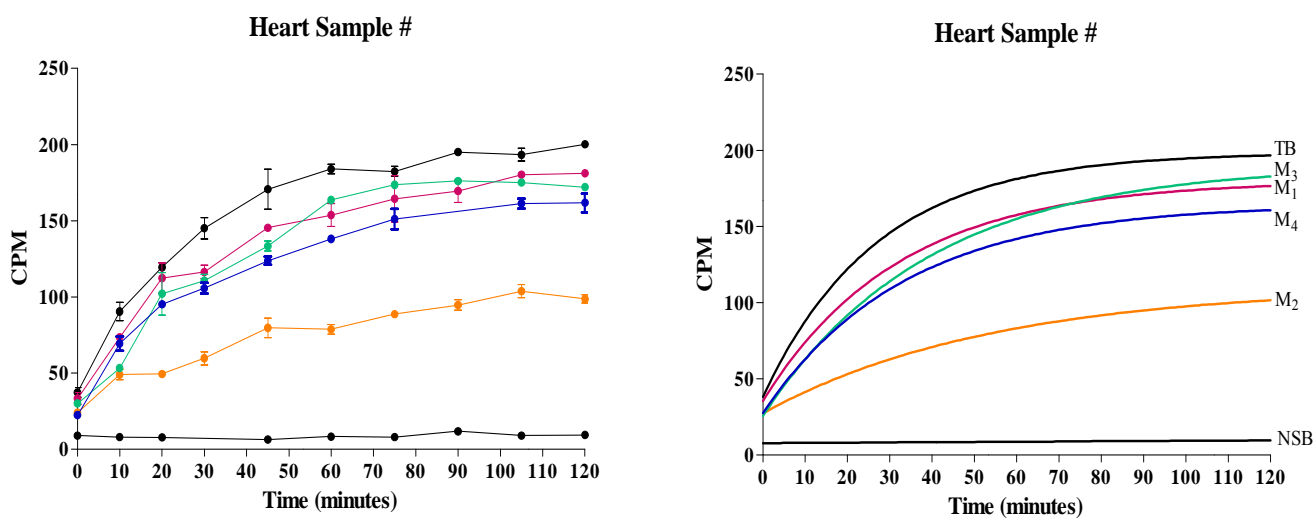


Figure 7. Saturation Curve for the Time-Dependent Competition Binding Assay. Percent binding of muscarinic subtypes were found by generating best-fit lines (shown on the right) from saturation curves (shown on the left). The values at the 2 hour time-point were fractionated from specific binding to determine results.

receptor subtype was therefore not measured in this study. Each antagonist was added at its established K_i value. K_i values were as follows (in M): Pirenzepine = 4.66×10^{-9} , Methoctramine = 6.18×10^{-8} pf-HHSiD = 1.92×10^{-8} , Tropicamide = 2.82×10^{-8} .

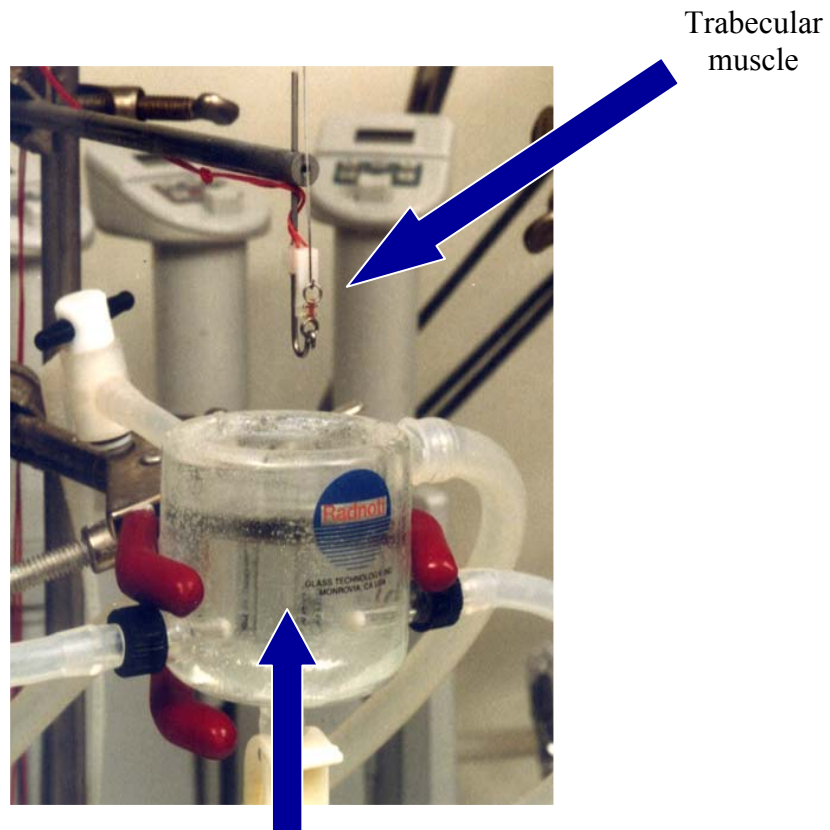
Holding radioactivity at 150pM per tube for all total binding, non-specific binding, and total count tubes, membrane (amount determined from membrane titer assay) was incubated in the presence of the selective antagonists. Tubes were mixed. Incubations were run in a shaking water bath at 37°C. Tubes were incubated at ten different time points (in minutes: 0, 10, 20, 30, 45, 60, 75, 90, 105, 120). Once complete, incubations were halted by placing tubes back into an ice water bath. Preparations were harvested, dried, and read as described in Section 2.4.

2.7 Muscle Function Experiments

Fresh trabecular muscles from non-failing, failing, and failing + LVAD tissues were used in this experiment. Tissue samples were collected from the operating room and placed in cold cardioplegia solution. Once in the lab, tissue samples were placed in an oxygenated petri dish filled with Krebs-Henseleit buffer (KHR) [composition in nM: 100 NaCl, 4.0 KCl, 1.5 $MgSO_4 \cdot 7H_2O$, 20.0 $NaHCO_3$, 1.5 NaH_2PO_4 , 20.0 Na-Acetate, 10.0 Glucose, 0.1 Ascorbic Acid, 2.5 $CaCl_2$, and 5.0 IU Insulin]. Up to 7 long, slender cylindrical muscles with a cross sectional area less than 1.1 mm^2 were dissected from the tissue. Each muscle was secured between two o-rings and transferred to the muscle experiment set-up.

A typical muscle experiment set-up is depicted in **Figure 8**. Each muscle is surrounded by a tissue bath filled with oxygenated KHR continuously heated at 37°C. Inside the bath, muscles are hung by two hooks and are in direct contact with platinum electrodes. These platinum wires send electrical stimuli (1Hz every 5msec) to the muscle via a stimulator. The stimulator controls the frequency, duration, and amount of voltage of each stimulus sent to the muscle. After the muscle is stimulated, the muscle produces tension in response to the stimulus, which is sensed by a force transducer. This sends the amount of force generated by the muscle to an amplifier which amplifies and conditions the signal and sends it to LabChart 7 Pro, a software program. Once on data acquisition software, results can be analyzed for six different contractile parameters. Contractile parameters analyzed are shown in **Figure 9**. These parameters include resting tension (RT), developed tension (DT), time to peak tension (TPT), time to half relaxation (THR), peak rate of tension rise (+dT/dt), and peak rate of tension fall (-dT/dt). RT is the tension produced by the muscle at rest and DT is the force produced by the muscle during contraction. TPT is the time it takes for the muscle to reach its peak of contraction and THR is the time it takes for the muscle to get from the peak of contraction to the halfway point of relaxation. dT/dt is the maximal rate of contraction (+dT/dt) or relaxation (-dT/dt).

Once hung on the set-up, each muscle remained in the bath for one hour without electrical stimulation. Muscles were then stimulated repeatedly for two minutes at 10V to reach a steady state of contraction. The threshold voltage was found by lowering



Tissue bath with Krebs-Henseleit

Figure 8. *Typical muscle bath set-up.* Each dissected muscle is secured between two o-rings and hung across a pair of platinum electrodes. Muscle baths are then lifted to surround the muscle with circulating, oxygenated Krebs-Henseleit buffer heated to 37°C.

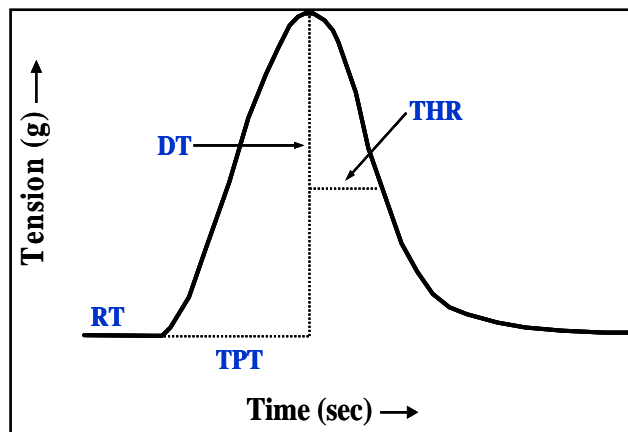


Figure 9. *Typical muscle contraction with contractile parameters.*

From an individual muscle contraction, determination of six contractile parameters are used to establish functionality, including resting tension (RT), developed tension (DT), time to peak tension (TPT), and time to half relaxation (THR). Peak rate of tension rise ($+dT/dt$) and peak rate of tension fall ($-dT/dt$) (not shown) are established at the steepest slope of the line leading to the peak of contraction and the steepest slope of the line leading back to RT.

voltage to 1V and increasing by 0.2V until the muscle began contracting. Upon contraction, voltage was increased by 20% which set the voltage for the remainder of the experiment.

A length-tension curve (LTC) was performed once muscles were contracting steadily at threshold voltage. Muscles were stretched by 0.1 mm. After one minute at the new length, DT and RT were recorded. These steps were repeated until DT stopped increasing upon stretch of the muscle to reach L_{max} (length associated with greatest muscle contraction). Setting each muscle to its L_{max} allowed for individual muscles to be compared to others. Once each reached L_{max}, muscles were left for 30 minutes to stabilize under these new conditions. After 30 minutes, muscles with DT \geq 0.20g were used for the experimental protocol.

Muscles were divided into two groups: those that received Acetylcholine (Ach) and those that served as time controls. A dose-response curve to Ach was performed. 1nM Ach was added only to the experiment group of muscles. After ten minutes, 10nM Ach was added. This series was repeated until six doses of Ach was added (1, 10, and 100nM, followed by 1, 10, and 100 μ M). After the last dose was added followed by the 10 minute rest, all muscles received 1 μ M isoproterenol.

Once the experimental protocol was complete, muscles were removed from KHR so the length between their o-rings could be measured. Once recorded, muscles were cut from the o-rings and placed in bibulous paper to dry. After drying for 15 minutes, individual muscles were weighed, so cross-sectional area (XSA) could be calculated.

$XSA = (\text{weight of muscle} / \text{length of muscle}) \div \text{density of muscle}$. RT, DT, +dT/dt, and -dT/dt were divided by XSA to normalize for muscle size.

Data recorded throughout the experiment was analyzed in order to draw conclusions.

2.8 Statistical Analysis

Total muscarinic receptor density and the percent of muscarinic receptor subtypes in non-failing, failing, and failing+LVAD tissue were analyzed using a one-way analysis of variance (ANOVA) and a Newman-Keuls post-hoc comparison test. Diagnoses (dilated cardiomyopathy versus ischemic cardiomyopathy) in failing and failing+LVAD groups were analyzed by a Kruskal-Wallis test followed by the Dunn's Multiple Comparison test. The Kruskal-Wallis test and Dunn's Multiple Comparison test was also used to determine total muscarinic receptor Kd changes between groups. Data is expressed as mean \pm SEM and significant differences were determined only when $p < 0.05$.

Baseline parameters in the muscle function experiments were analyzed using an unpaired t-test if the parameter passed a normality test or a Mann Whitney test if the parameter did not pass a normality test. Dose-response curves were analyzed by a two-way ANOVA followed by the Bonferroni post-test. A two-way ANOVA and Bonferroni post-test was also used to determine the response of muscles upon the addition of isoproterenol. Data is expressed as the mean \pm SEM for baseline parameters, mean percent change from baseline for dose-response curves, and mean percent change from the last dose of acetylcholine for isoproterenol data. Significant differences were determined only when $p < 0.05$.

CHAPTER III

RESULTS

3.1 Total Muscarinic Receptor Density and Affinity

Table I shows the patient population used to measure muscarinic receptors (all = total; highlighted in grey = subtypes; **Table I** on page 32, description of **Table I** on page 33). Patients of both sexes were included in the study and sample groups were chosen to have a similar age (in mean \pm SD; NF = 49 ± 5 , F = 51 ± 5 , and F+LVAD = 52 ± 8). Because ejection fractions $\geq 50\%$ are a marker of normal cardiac function, NF samples only with ejection fractions $\geq 50\%$ were included. F and F+LVAD samples had ejection fractions $\leq 50\%$. Exclusion criteria was also considered, therefore patients on pacemakers or on drugs with potential muscarinic interactions were excluded from the study. Common medications taken by the patient population are included in **Table I**, with patients most commonly on β -blockers, angiotensin converting enzyme (ACE) inhibitors, and inotropes. Sixty-one total left ventricular samples were used to measure total muscarinic

Patient #	Diagnosis	Age	Sex	Ejection Fraction	Medications
1	NF	60	F	65	DOB, NE
2	NF	54	F	N/A	NE
3	NF	42	M	N/A	DOP
4	NF	53	F	50	DOP, EN
5	NF	44	M	75-80	DOP
6	NF	50	M	60	DOB
7	NF	44	F	55-60	DOP, NE
8	NF	50	M	70	N/A
9	NF	50	F	65-70	DOP, NE
10	NF	48	F	50-55	DOP
11	NF	55	F	60	DOP
12	NF	46	F	70	NE
13	NF	56	F	65	DOP, EN
14	NF	47	F	50	DOP
15	NF	40	M	60	DOP
16	F-DCM	40	M	10	NE
17	F-DCM	48	F	15	CARV, DIG, LIS
18	F-DCM	54	M	15	LOS
19	F-DCM	56	F	25	CARV, LIS, MIL
20	F-DCM	47	M	30	LIS, MET
21	F-DCM	45	M	10	LIS, MIL
22	F-DCM	49	F	30	N/A
23	F-DCM	53	F	15	CARV, DIG, DOB, DOP, MIL, NE
24	F-DCM	46	M	15	CARV
25	F-DCM	53	F	20	CARV, MIL
26	F-DCM	41	M	10	CARV
27	F-DCM	50	M	10	DOP
28	F-DCM	52	F	10	CARV, DIG
29	F-DCM	45	F	15	CARV
30	F-DCM	52	M	25	DIG, LIS, MET
31	F-ICM	56	F	15	LIS, MET
32	F-ICM	60	F	25	CARV
33	F-ICM	52	M	24	CARV
34	F-ICM	58	M	15	MET, MIL
35	F-ICM	53	M	35	CARV, DIG, VAL
36	F-ICM	52	M	15	DIG, MIL
37	F-ICM	56	M	15	CARV, MIL
38	F-ICM	43	F	30	CARV, MIS
39	F-ICM	53	M	15	MIL
40	F-ICM	55	F	15-20	CARV
41	F-ICM	48	M	20	LIS
42	F-ICM	54	F	10	DIG
43	F-ICM	58	F	35	N/A
44	F-ICM	58	M	20	CARV
45	F-ICM	55	F	20	DIG
46	F+LVAD	42	M	15	EN
47	F+LVAD	50	M	10	N/A
48	F+LVAD	43	M	15	DIG
49	F+LVAD	59	M	10	N/A
50	F+LVAD	54	M	15	DOB, DOP, EPI, NE
51	F+LVAD	53	F	10	N/A
52	F+LVAD	51	M	15	DOB
53	F+LVAD	44	M	10	DOB
54	F+LVAD	43	M	N/A	MET
55	F+LVAD	39	M	10	CARV, DIG, DOP
56	F+LVAD	62	M	50	DIG
57	F+LVAD	62	F	15	N/A
58	F+LVAD	54	M	20	CARV, LIS
59	F+LVAD	65	M	25	N/A
60	F+LVAD	65	M	20	CARV, LIS
61	F+LVAD	49	M	10	LIS, MET

Table I. *Characteristics of Patients Used to Measure Total and Subtyped Muscarinic Receptors.* Sixty-one human left ventricular samples were used to measure total muscarinic receptor density and 36 of these samples (highlighted in grey) were also used to measure the percent of M1-M4 receptor subtypes. Patients in each diagnosis were chosen with similar ages and both males and females were used in the study. Ejection fractions in NF tissue needed to be $\geq 50\%$ and in F and F+LVAD tissue $\leq 35\%$ to be included in the study. Common medications are also listed. (Abbreviations: DOB = Dobutamine, NE = Norepinephrine, DOP = Dopamine, EN = Enalapril, CARV = Carvedilol, DIG = Digoxin, LIS = Lisinopril, LOS = Losartan, MIL = Milrinone, MET = Metoprolol, EPI = Epinephrine, VAL = Valsartan)

receptor density and 36 of these samples were also used to measure the percents of muscarinic receptor subtypes.

Before measuring total muscarinic receptor density on all 61 left ventricular samples, positive controls were measured to ensure valid experimental technique. It is established that there are a more dense population of muscarinic receptors in atrial tissue compared to ventricular tissue and there are even greater densities in the brain than in the atria or ventricles^{22,44}. Using my established radioligand binding assay protocol, I measured receptor densities on left ventricular and right atrial tissue (n=3 per group) from the same hearts and from one piece of un-identified brain tissue. **Figure 10** shows that the lowest muscarinic receptor density was measured in the three left ventricular samples (332.70 ± 35.90 fmol/mg). The three hearts had a higher density in the right atrium, with densities of 571.70 ± 93.78 fmol/mg. The brain tissue had receptor densities of 1029 fmol/mg protein. The positive controls mimicking data in the literature supported the experimental protocol we established, therefore the 61 project samples could be successfully measured.

Figure 11 shows the results of the radioligand binding assays on the 61 project samples. The 15 NF samples were found to have receptor densities of 194.10 ± 17.27 , F samples 275.80 ± 11.89 , and F+LVAD samples 315.80 ± 23.94 (all in fmol/mg protein). The F group was found to be significantly increased compared to control group ($p < 0.01$) and F+LVAD group was even more significantly increased compared to control ($p < 0.001$). Because the F and F+LVAD groups contained samples with a diagnosis of

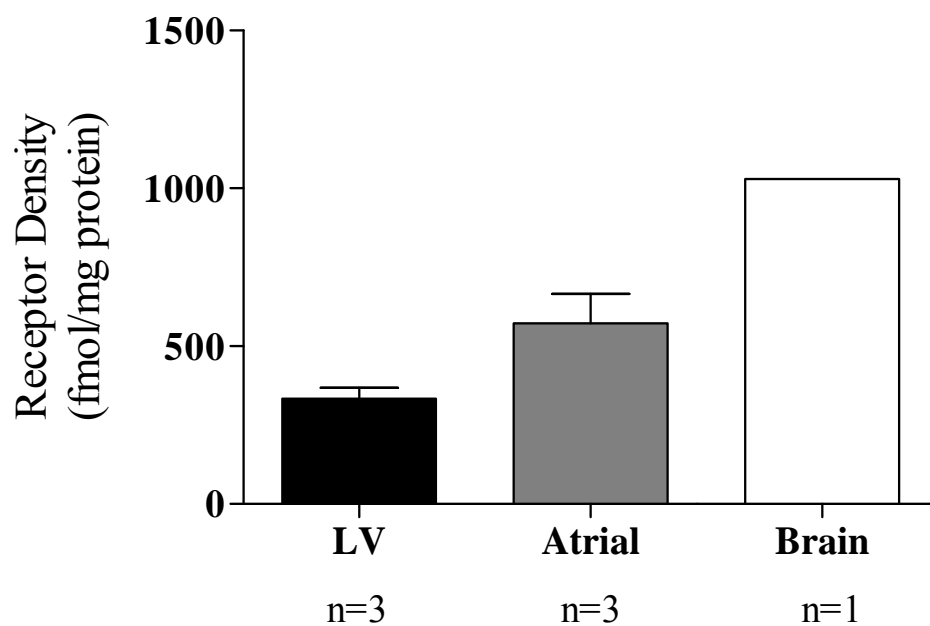


Figure 10. Positive Control Experiment. Right atrial and left ventricular (LV) tissue was taken from the same 3 hearts (from patients undergoing cardiac transplantation) and one piece of un-identified brain tissue was acquired from pathology to measure total muscarinic receptor densities.

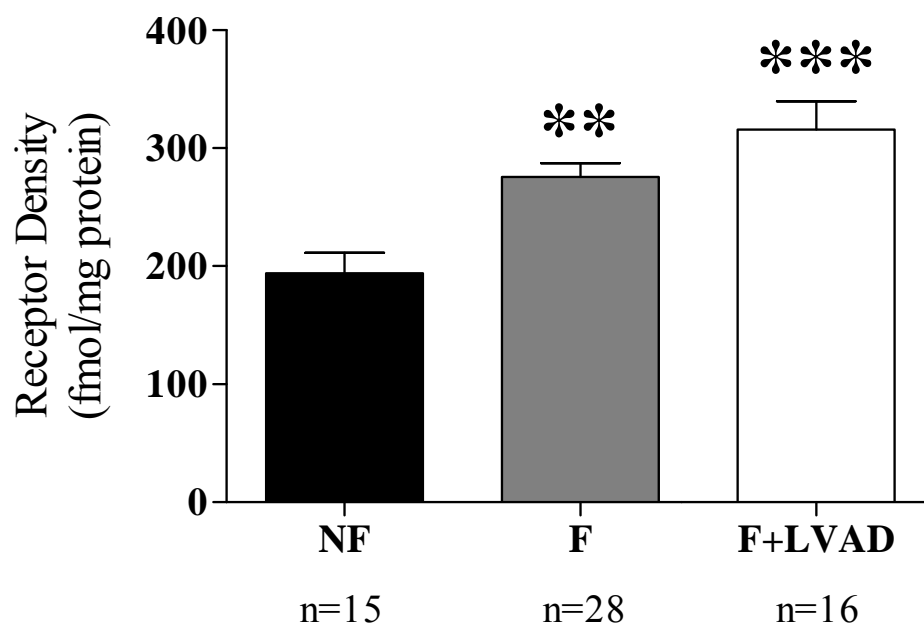


Figure 11. Total Muscarinic Receptor Density. A 1-way ANOVA detected a significant increase in total muscarinic receptor density in F samples compared to control ($p < 0.01$) and an even more significant increase in receptor density in F+LVAD samples versus control ($p < 0.001$).

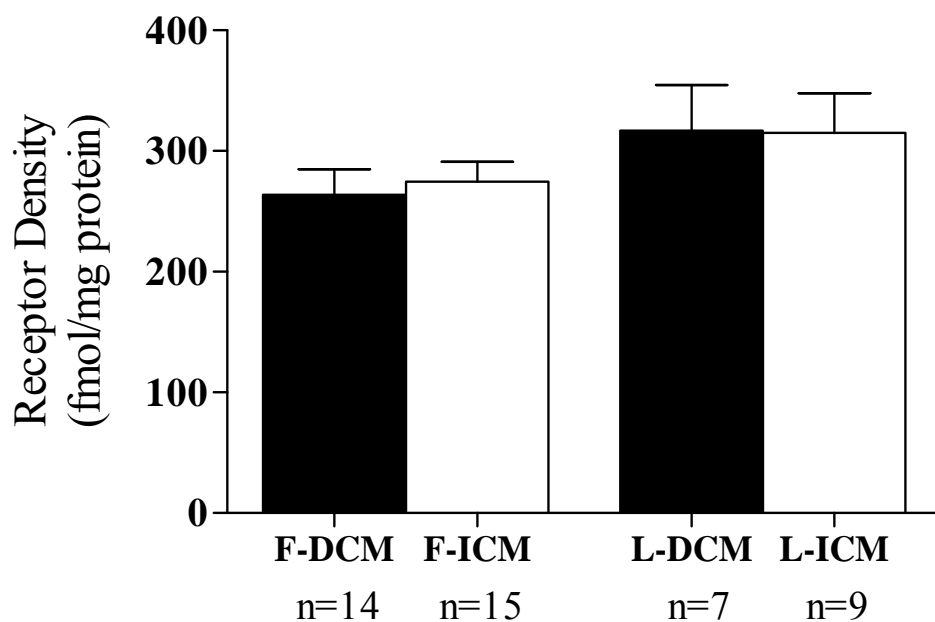


Figure 12. Relationship of Muscarinic Receptor Densities to Patient Diagnosis. Total muscarinic receptor density comparisons were made between DCM and ICM diagnoses in F patients and patients with LVAD support. A statistical analysis was performed and found no significant differences in density between etiologies ($p=0.698$). L-DCM and L-ICM densities were also unchanged between groups ($p=0.974$). (Abbreviations: DCM = Dilated Cardiomyopathy; ICM = Ischemic Cardiomyopathy; L = F+LVAD group)

both DCM and ICM, I wanted to see if various diagnoses of HF resulted in different muscarinic receptor densities. As shown in **Figure 12**, when separating the F group into F-DCM and F-ICM, receptor densities were unchanged (263.90 ± 20.98 versus 274.40 ± 16.80). Densities were also not significantly different when the F+LVAD group was separated into diagnoses (316.70 ± 38.03 versus 315.00 ± 32.66). Groups were further divided into male versus female to see if gender had an effect on muscarinic receptor densities (F+LVAD group was not analyzed this way due to the uneven distribution of males and females). A t-test was run to compare males to females in the NF group and males to females in the F group, as shown in **Figure 13**. No significant differences were found in the NF group, with females (n=10) having densities of 180.3 ± 17.9 fmol/mg protein and males (n=5) with densities of 221.9 ± 37.4 fmol/mg protein. The F group also showed no significant changes in receptor densities, with the mean density in females (n=13) 289.9 ± 18.8 fmol/mg and males (n=16) 252.6 ± 17.7 fmol/mg protein.

LVADs, although all implantable pumps that hemodynamically unload the heart, have developed into different types and are implanted for varying amounts of time from patient to patient. Because of these factors, the type of LVAD was compared to see if muscarinic receptor densities changed from LVAD type. **Figure 14** compares muscarinic receptor densities in different LVAD types. A Mann-Whitney analysis was performed and found no significant changes in receptor density between pulsatile (284.5 ± 33.1 fmol/mg) and non-pulsatile (334.5 ± 32.6 fmol/mg) LVADs. **Figure 15** compares the duration of time patients were supported with an LVAD to their found muscarinic

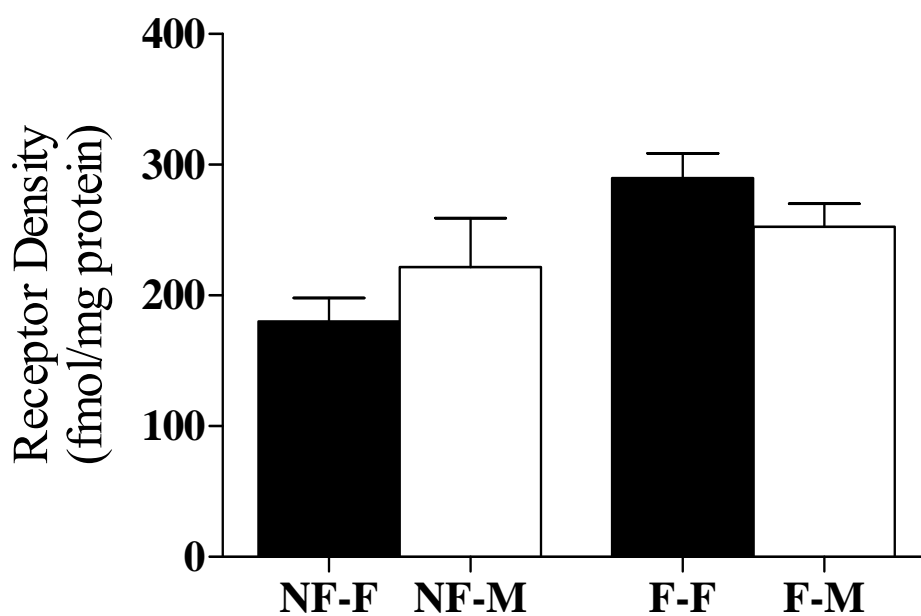


Figure 13. Gender Comparisons Between NF and F Muscarinic Receptor Densities. NF and F muscarinic receptor densities were separated into male (M) and female (F) groups to see if differences in muscarinic receptor densities occurred with gender differences. No significant changes in densities were detected by t-test analysis for the NF ($p=0.271$) and F ($p=0.162$) groups.

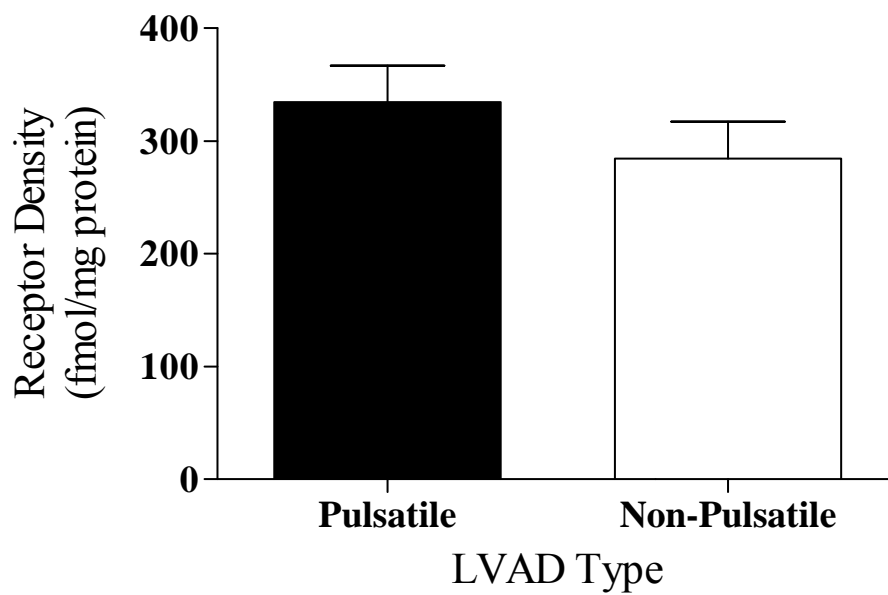


Figure 14. *Total Muscarinic Receptor Densities in Different LVAD Types.* Two types of LVADs, pulsatile and non-pulsatile, were found to have no significant effect on muscarinic receptor densities through a Mann-Whitney statistical analysis ($p=0.368$).

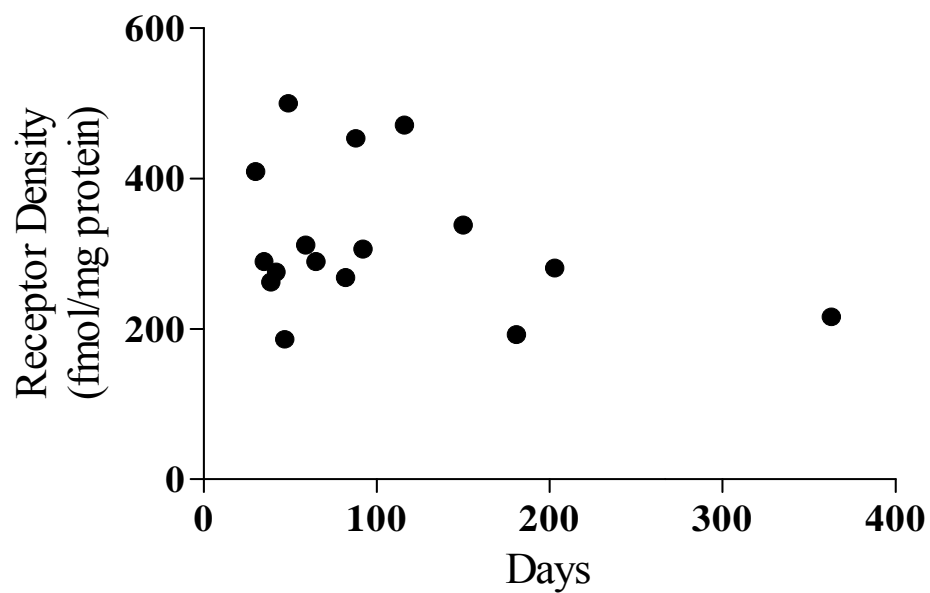


Figure 15. *Relationship between duration of LVAD Support and Total Muscarinic Receptor Density.* The amount of time patients were on LVAD support was compared to their found muscarinic receptor densities. No significant correlation was detected between the days on LVAD support to receptor density ($p=0.260$).

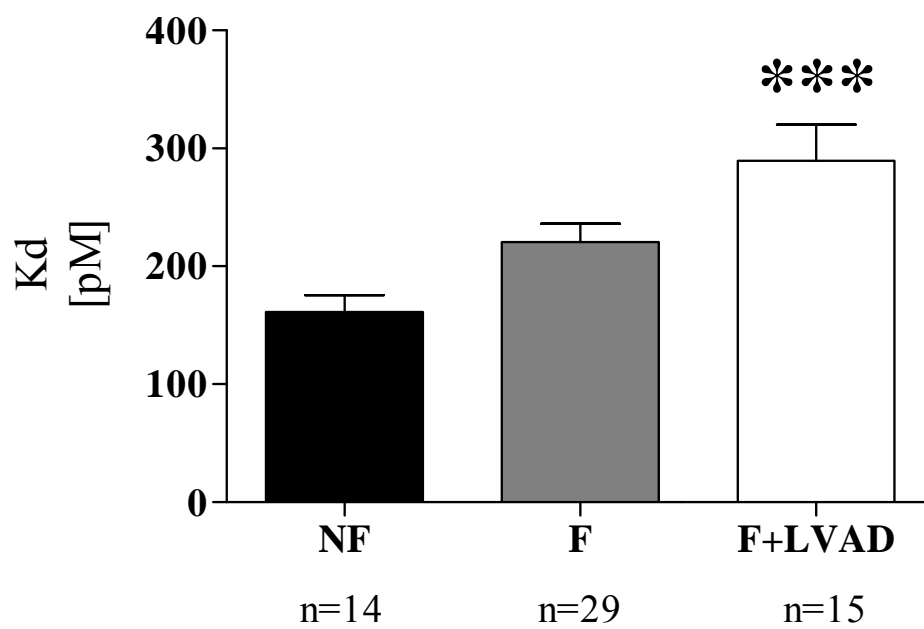


Figure 16. Muscarinic Receptor Kd. Kd values were found in the radioligand binding assays. A 1-way ANOVA found no significant change in Kd from NF to F samples. A significant increase in Kd was found in the F+LVAD group versus control ($p < 0.001$).

receptor densities. Statistical analysis found no significant correlation between the days of LVAD support and receptor densities.

The radioligand binding assays measured total muscarinic receptor density as well as receptor K_d. The K_ds found for the three groups are depicted in **Figure 16**. No significant differences were found when comparing NF and F groups, with K_ds of 220.40 ± 15.88 pM in F versus 161.10 ± 14.54 pM in control. The F+LVAD group had K_ds of 289.40 ± 30.92 pM, resulting in a statistically significant increase in K_d versus control.

3.2 Percents of Muscarinic Receptor Subtypes in NF, F, and F+LVAD Tissue

Muscarinic receptor subtypes were measured in NF, F, and F+LVAD left ventricular tissue. Thirty-six of the samples used to measure total muscarinic receptor densities were also used to measure percents of muscarinic receptor subtypes using the time-dependent competition binding assay (tissue from patients highlighted in grey on **Table I**). Once all data was collected, the percent of each subtype was compared. The raw data results for each subtype are depicted in **Figures 17-20**. The percent of M₁ subtype, as shown in **Figure 17**, was 15.63 ± 3.11 in NF tissue, 12.96 ± 3.15 in F, and 21.28 ± 1.96 in F+LVAD. Although the percent of M₁ appears to be lower in failure and increase back up upon LVAD support, the differences did not reach statistical significance. The percent of muscarinic receptor subtype M₂ also did not change from NF to F or F+LVAD. With percents of 61.60 ± 2.93 (NF), 60.19 ± 1.82 (F), and 62.86 ± 2.25 (F+LVAD), depicted in **Figure 18**, the percent of M_{2S} stayed the same in each group. **Figure 19** shows the results of M₃. The percent of M₃ was 19.83 ± 3.73 in NF, 10.97 ±

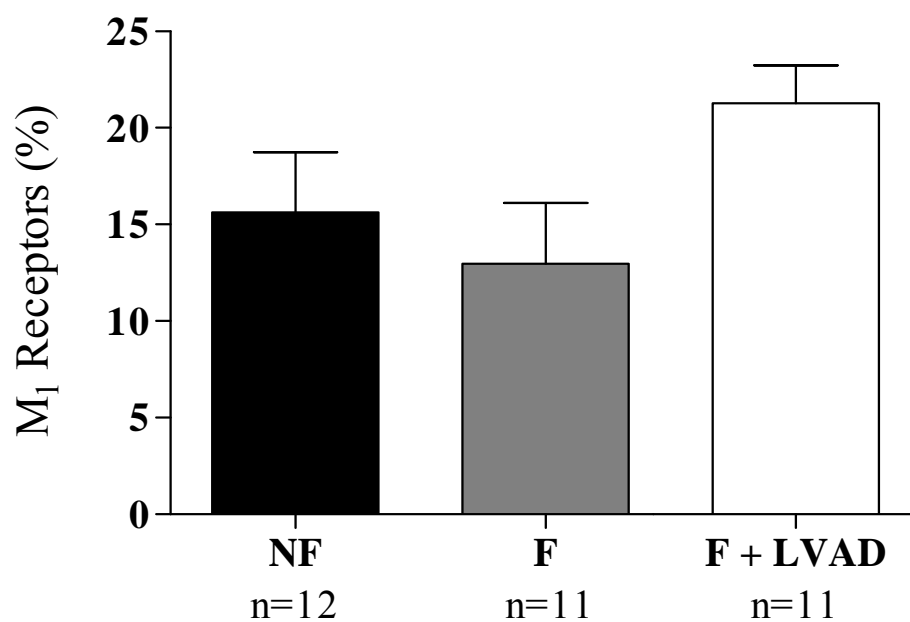


Figure 17. Percents of M₁ Receptor Subtype (Raw Data). Before normalizing to 100%, a 1-way ANOVA detected no significant changes in the percents of M₁ found in each group (p=0.127).

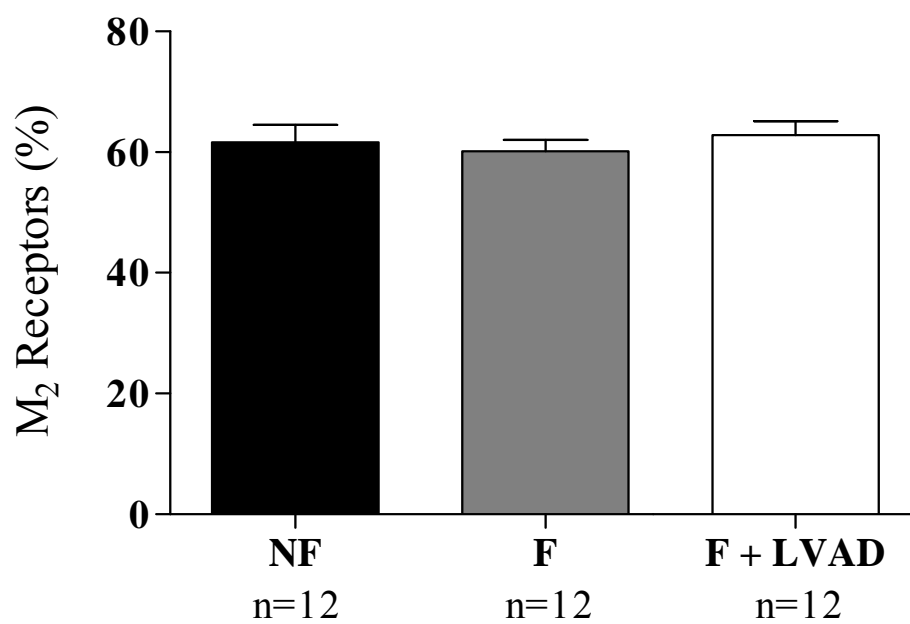


Figure 18. *Percents of M₂ Receptor Subtype (Raw Data).* Before normalizing to 100%, a 1-way ANOVA detected no significant changes in the percents of M₂ found in each group (p=0.730).

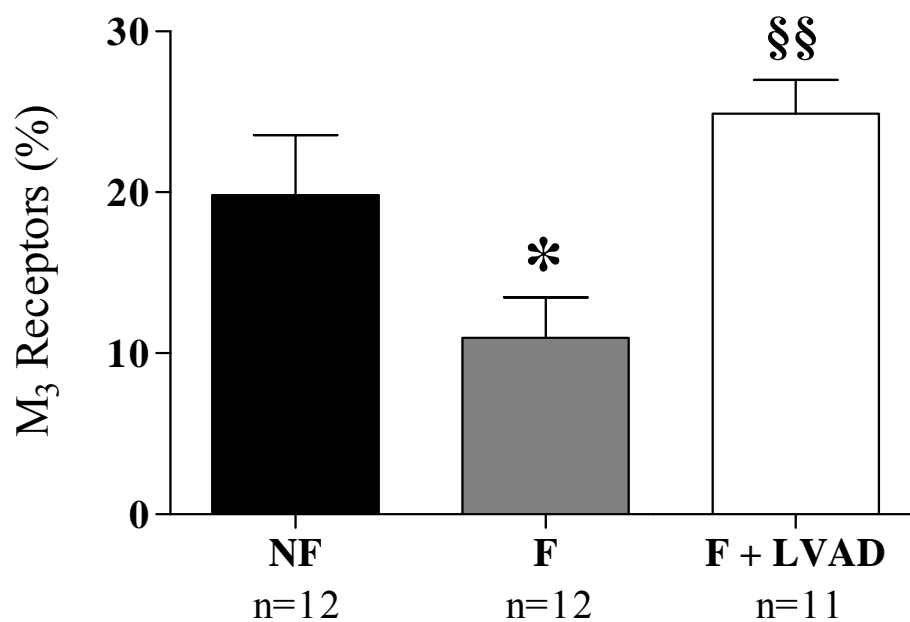


Figure 19. Percents of M₃ Receptor Subtype (Raw Data).

Before normalizing to 100%, a 1-way ANOVA detected a significant decrease in the percent of M₃ receptor subtype in F tissue compared to control (* p<0.05). A significant increase was found in the F+LVAD group versus the F group (§§ p<0.01).

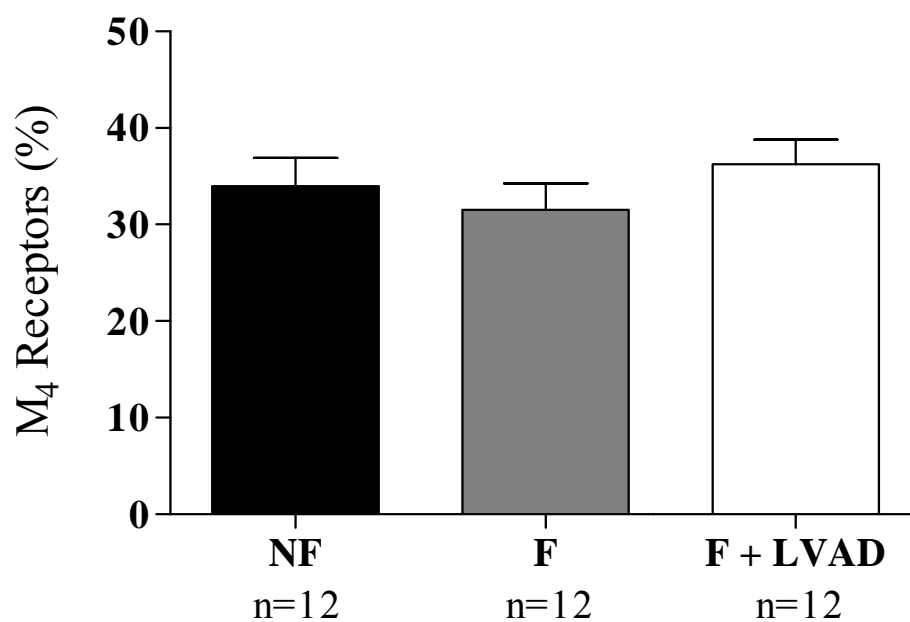


Figure 20. *Percents of M₄ Receptor Subtype (Raw Data).*

Before normalizing to 100%, a 1-way ANOVA was performed and detected no significant changes in the percents of M₄ found in each group (p=0.495).

2.52 in F, and 24.89 ± 2.09 in F+LVAD. The percent of M_3 did significantly decrease from NF to F ($p < 0.05$) and increase back up from F to F+LVAD ($p < 0.01$). The percents of M_4 did not significantly change between the three groups. As shown in **Figure 20**, the percents of M_4 were 33.97 ± 2.93 in NF, 31.53 ± 2.75 in F, and 36.21 ± 2.60 in F+LVAD.

On a heart to heart analysis, the percents of M_1 , M_2 , M_3 , and M_4 equated to a value not equal to 100%. This was not a surprising find due to the four subtype selective antagonists not being absolutely subtype selective. Because of this, it was also important to normalize each heart to 100% and compare the results to the raw data. **Figure 21** shows the percents of M_1 once data was normalized to 100%. With percents of 12.03 ± 1.33 in NF, 9.97 ± 1.95 in F, and 14.47 ± 1.11 in F+LVAD, no statistically significant differences were found between groups. Looking at the raw percents of M_1 in **Figure 17** and the normalized graph in **Figure 21**, both sets of data show a slight loss in failure and increase back upon LVAD support. **Figure 22**, the normalized percents of M_2 , show 49.29 ± 2.75 in NF, 53.34 ± 3.29 in F, and 43.75 ± 1.20 in F+LVAD. Like the raw data in **Figure 18**, no significant differences were found when comparing NF and F groups. A difference only detected in the normalized data was the decrease in percent M_2 upon LVAD support compared to the percent in failure ($p < 0.05$). The percent of M_3 s once normalize, in **Figure 23**, revealed the same results as the raw data. There was a significant decrease in the percent M_3 in F (8.61 ± 1.65) versus NF (13.56 ± 2.16) with recovery from failure upon LVAD support (16.65 ± 0.72). The percents of M_4 s normalized also showed the same results as the raw results. **Figure 24** shows the results with 25.19 ± 0.93 in NF, 26.41 ± 0.67 in F, and 25.83 ± 1.37 in F+LVAD.

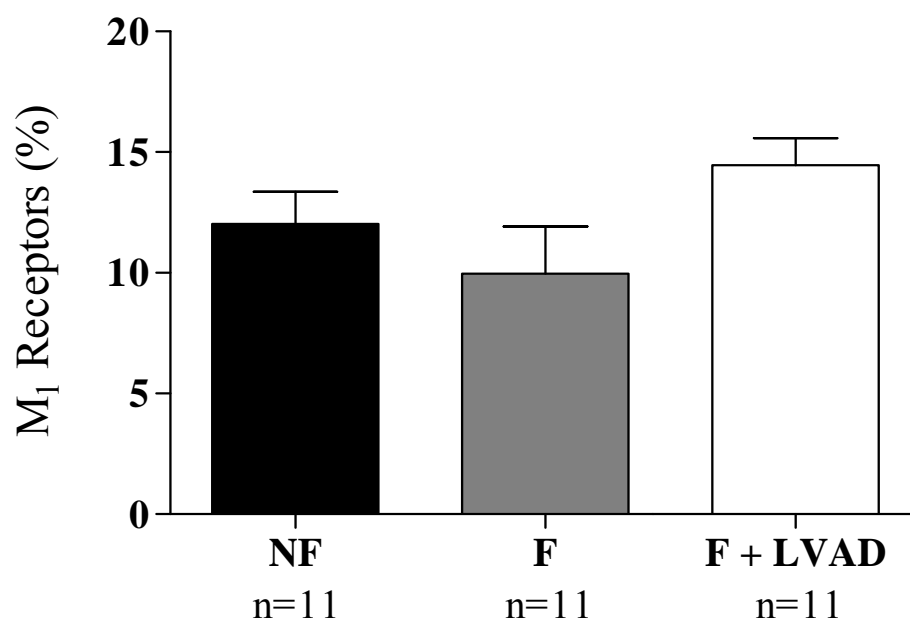


Figure 21. *Percents of M₁ Receptor Subtype (Normalized Data).* After normalizing to 100%, a 1-way ANOVA was performed and detected no significant changes in the percents of M₁ found in each group (p=0.124).

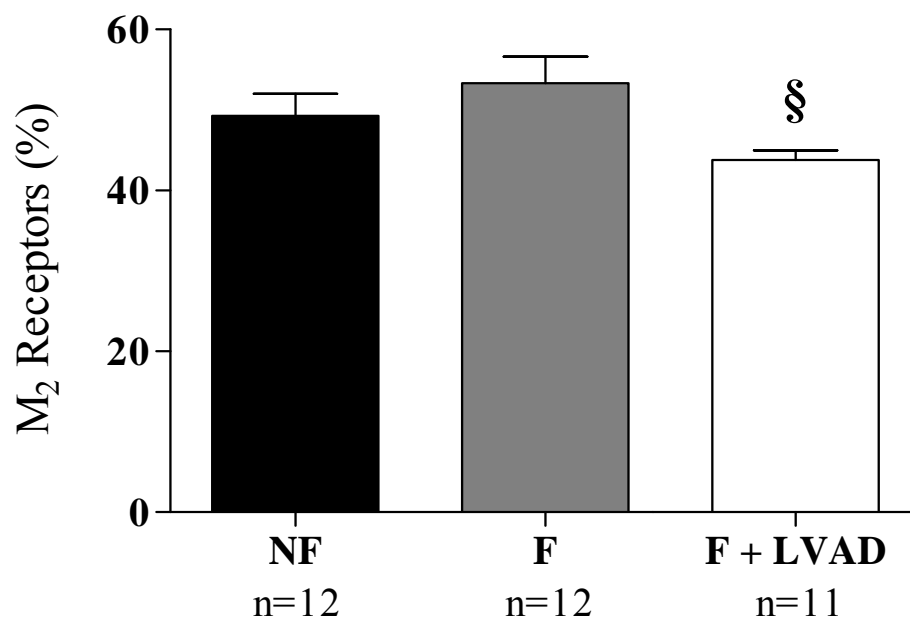


Figure 22. Percents of M₂ Receptor Subtype (Normalized Data). After normalizing to 100%, a 1-way ANOVA was performed and detected no significant changes in the percents of M₂ from F to NF tissue. A significant decrease in the percent M₂ receptor subtype was found in the F+LVAD group versus the F group ([§] p<0.05).

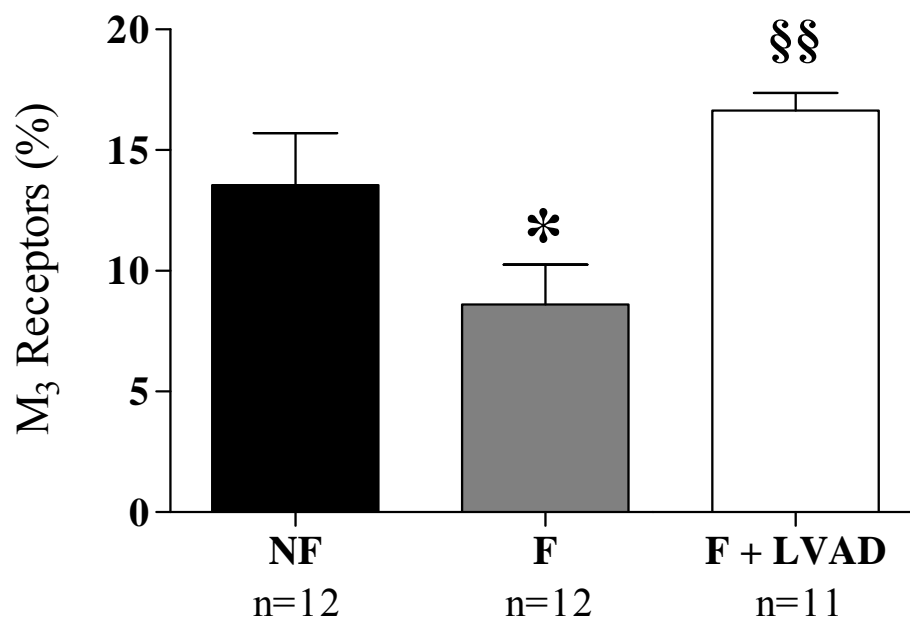


Figure 23. Percents of M₃ Receptor Subtype (Normalized Data).

After normalizing to 100%, a 1-way ANOVA detected a significant decrease in the percent of receptor subtype M₃ in the F group versus control (* p<0.05) and a significant increase in the percent of receptor subtype M₃ in the F+LVAD group versus the F group (§§ p<0.01).

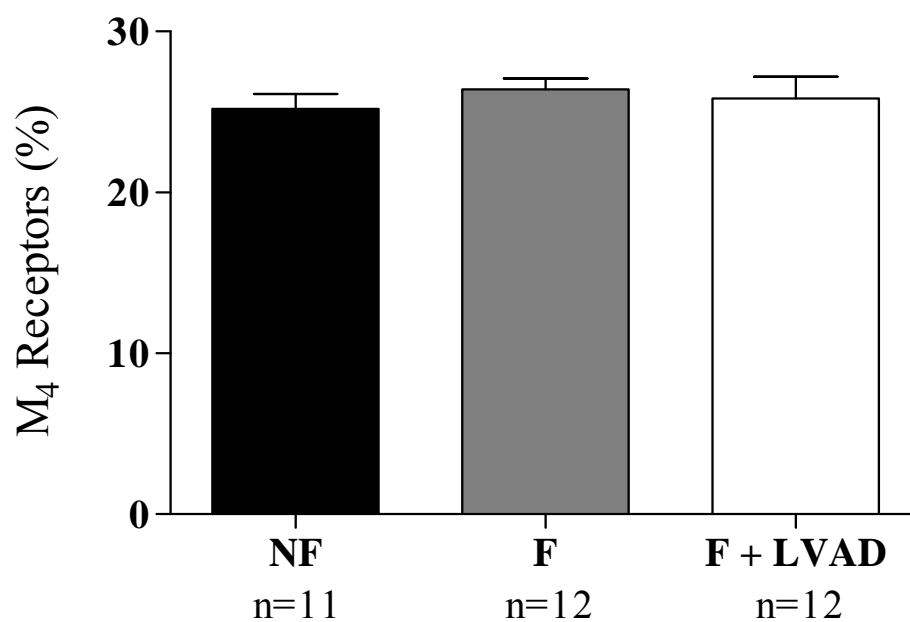


Figure 24. Percents of M₄ Receptor Subtype (Normalized Data). After normalizing to 100%, a 1-way ANOVA was performed and detected no significant changes in the percents of M₄ found in each group (p=0.714).

It was difficult to make conclusions about each receptor subtype in failure and with mechanical unloading for several reasons. First, the technique used only produced the percent of each subtype in LV samples, not the density. While making conclusions about the percent of each subtype is sufficient, the potential change in subtype density may not mirror the same differences. Also, the lack of absolutely subtype selective antagonists for these subtypes made it more difficult to interpret the data. Because M_1 and M_3 subtypes couple to the same G protein and stimulate the same signaling pathway, the percent of these two subtypes together were also determined for each group. **Figure 25** shows these results. It was found that the percent of $M_1 + M_3$ was 26.82 ± 2.28 in NF, 20.25 ± 2.94 in F, and 31.11 ± 1.35 in F+LVAD. The percent of these odd-numbered subtypes did not significantly change in failure versus control. Upon LVAD support, the percent of $M_1 + M_3$ significantly increased versus failure. M_2 and M_4 couple to the same G protein and stimulate the same signaling pathway, therefore the percent of these subtypes together were also determined for each group. as shown in **Figure 26**, the percent of $M_2 + M_4$ were 73.24 ± 2.31 in NF, 79.75 ± 2.94 in F, and 68.89 ± 1.35 in F+LVAD. No significant differences were found between NF and F groups. Upon LVAD support, there was a significant decrease in the percent of $M_2 + M_4$ versus the percent in failure.

3.3 Muscle Function Analysis

Table II shows the patient population used to study muscle function on fresh cardiac muscles of the left ventricle. Twenty patients were used, including 11 representing NF

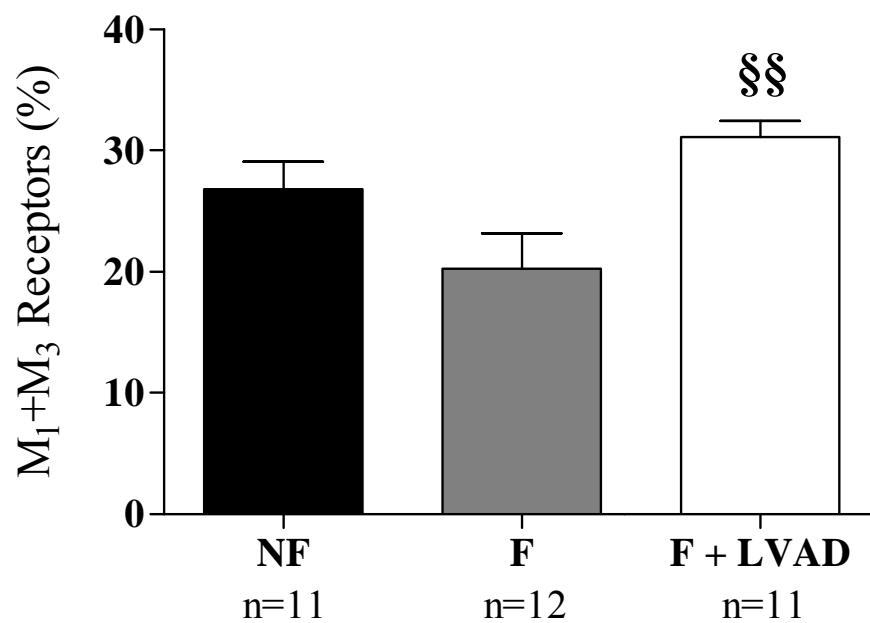


Figure 25. Percents of M_1 and M_3 Receptor Subtypes. M_1 and M_3 receptor subtypes couple to Gq proteins to elicit the same downstream signaling pathway. Percents of these odd-numbered subtypes were added together on a heart-by-heart basis and a 1-way ANOVA found no significant change in these receptor subtypes in F tissue versus NF tissue, but a significant increase in F+LVAD versus F tissue (§§ $p < 0.01$).

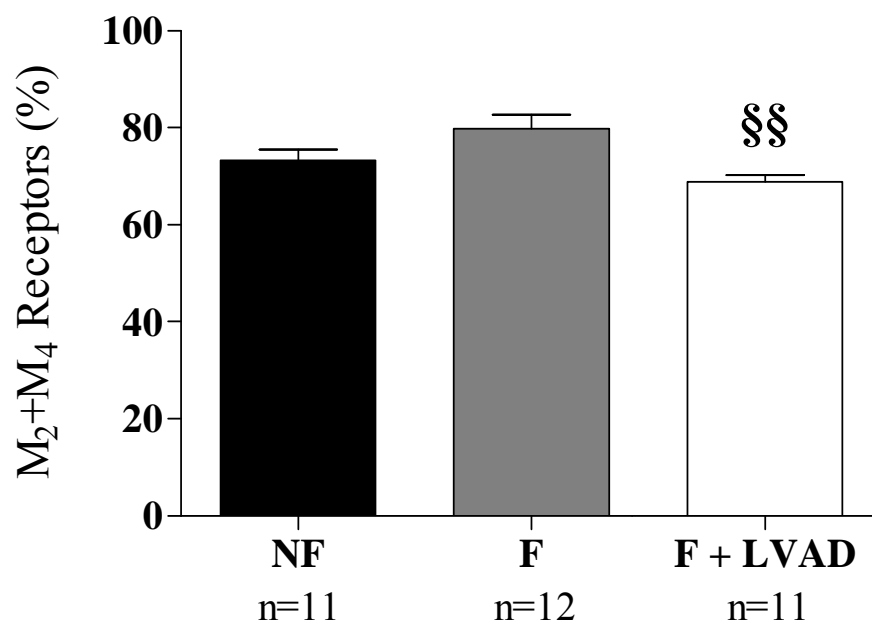


Figure 26. Percents of M_2 and M_4 Receptor Subtypes. M_2 and M_4 receptor subtypes couple to G_i proteins to elicit the same downstream signaling pathway. Percents of these even-numbered subtypes were added together on a heart-by-heart basis, and a 1-way ANOVA found no significant change in these receptor subtypes in F tissue versus NF tissue, but a significant decrease in F+LVAD versus F tissue (§§ $p < 0.01$).

Patient #	Diagnosis	Age	Sex	Ejection Fraction	Medications
1	NF	64	F	65	MET, CAP
2	NF	61	F	72	AM, MET
3	NF	42	M	55	MET
4	NF	71	F	65	MET
5	NF	39	M	70	N/A
6	NF	47	M	65	AM, MET
7	NF	54	M	60	MET
8	NF	53	F	65	MET
9	NF	74	F	63	LIS
10	NF	72	F	63	MET
11	NF	41	M	59	N/A
12	F-DCM	56	M	15	DIG, MIL
13	F-ICM	60	M	15	AM, DIG, EPI, MIL
14	F-ICM	50	M	20	CARV, DIG, LIS, MIL
15	F-DCM	46	M	25	AM, LIS, MIL
16	F-ICM	67	M	10	AM, CARV
17	F-DCM	58	M	20	DIG, CARV, LIS
18	F-DCM	68	M	10	AM, NE, LIS, MET
19	F-DCM	63	F	20	DIG, MIL
20	F-DCM	48	F	20	CARV, DIG, LIS

Table II. *Characteristics of Patients Used in Muscle Function Studies.*

Left ventricular (LV) tissue samples were taken from 20 patients, 11 representing NF tissue and 9 representing F tissue. Ages ranged from 39-74 years with both males (M) and females (F) included in the experiment. Ejection fractions needed to be $\geq 50\%$ in the NF tissue and $\leq 35\%$ in the F group. Common medications taken by each patient are listed above. (Abbreviations: MET = Metoprolol, CAP = Captopril, AM = Amiodarone, LIS = Lisinopril, DIG = Digoxin, EPI = Epinephrine, MIL = Milrinone, CARV = Carvedilol, NE = Norepinephrine)

tissue and 9 HF patients. The ages of patients studied ranged from 39-74 years old with both males and females included in the study. Ejection fractions were greater than 50% in all NF tissue and less than 35% in HF patients. Common medications used by each patient included β -blockers, ACE inhibitors, and inotropes.

Before adding acetylcholine (ACh) or isoproterenol (ISO) to the muscles, the six contractile parameters were recorded for both time control and drug-treated muscles.

Table III and **Table IV** represent the baseline results. When comparing all NF muscles (time control and ACh-treated) to F muscles (time control and ACh-treated), initial differences were found in developed tension, time to peak tension, and time to half relaxation. This is not surprising because failing tissue has been found to have less contractile abilities than non-diseased cardiac tissue. **Table IV** compares the baseline contractile parameters of time control versus ACh-treated muscles in each group. No differences were found for any of the six contractile parameters. This baseline data ensures that differences found between time control and drug-treated muscles was due strictly to the doses of ACh or ISO and not by differences in quality of the muscle.

Dose-Response Curves Upon Additions of ACh

The contractile parameters were recorded after addition of each ACh dose. For each parameter, comparisons were made between time control and ACh muscles in each sample group and comparing the addition of ACh between NF and F groups.

Figure 27 shows the resting tension (RT) results with addition of ACh. At all six doses, no significant differences were found when comparing NF time control to NF ACh-treated, F time control to F ACh-treated, or NF ACh-treated to F ACh-treated.

Contractile Parameters	NF	F
RT (g/mm²)	2.15 ± 0.25	2.36 ± 0.18
DT (g/mm²)	1.46 ± 0.21	0.91 ± 0.12*
TPT (msec)	242.20 ± 4.54	168.10 ± 8.20***
THR (msec)	137.20 ± 2.43	120.6 ± 3.09***
+dT/dT (g/sec/mm²)	13.29 ± 1.77	13.22 ± 1.77
-dT/dt (g/sec/mm²)	-13.31 ± 1.80	-11.83 ± 1.87

Table III. *Baseline Contractile Parameters in NF and F Muscles.*

Baseline contractile parameters were compared in NF and F tissue groups. no significant changes in RT, +dT/dt, or -dT/dt were detected from F to NF groups. Significant decreases were found in DT (p<0.05), TPT (p<0.001), and THR (p<0.001) in failure versus non-diseased tissue.

Contractile Parameters	NF - TC	NF - ACh	F - TC	F - ACh
RT (g/mm²)	2.25 ± 0.37	1.99 ± 0.29	2.39 ± 0.27	2.23 ± 0.26
DT (g/mm²)	1.78 ± 0.30	1.17 ± 0.18	0.89 ± 0.21	0.87 ± 0.11
TPT (msec)	247.80 ± 7.67	239.40 ± 4.50	170.50 ± 9.15	166.30 ± 8.65
THR (msec)	139.70 ± 2.24	135.10 ± 3.60	125.30 ± 4.95	120.00 ± 3.23
+dT/dT (g/sec/mm²)	13.14 ± 1.43	12.85 ± 2.44	11.12 ± 2.10	12.23 ± 1.18
-dT/dt (g/sec/mm²)	-13.16 ± 1.56	-13.00 ± 2.57	-9.53 ± 2.11	-10.84 ± 1.21

Table IV. Baseline Contractile Parameters in Muscles to be Treated with ACh and Those Muscles Serving as Time Control (TC). NF and F tissue was divided into muscles that would be treated with doses of ACh and those to serve as a control. Before the experiment, contractile parameters were compared between the ACh-treated muscles and TC muscles in both tissue types. No significant differences were found in either tissue group.

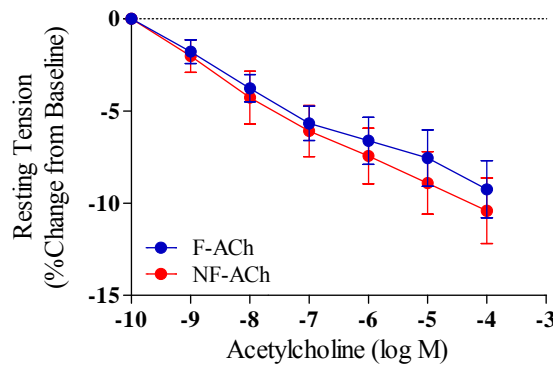
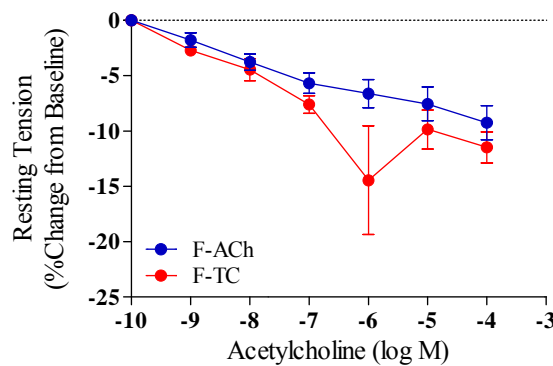
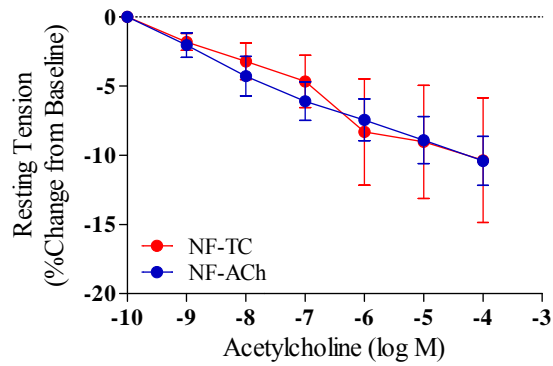


Figure 27. Dose-Response to ACh – Resting Tension (RT) Results.

No significant changes were found between NF muscles treated with ACh and those serving as time control (TC) [top graph]. No significant changes were found between F muscles treated with ACh and those serving as TC [middle graph]. No significant differences were detected in the percent change of RT in ACh-treated F muscles versus ACh-treated NF muscles [bottom graph].

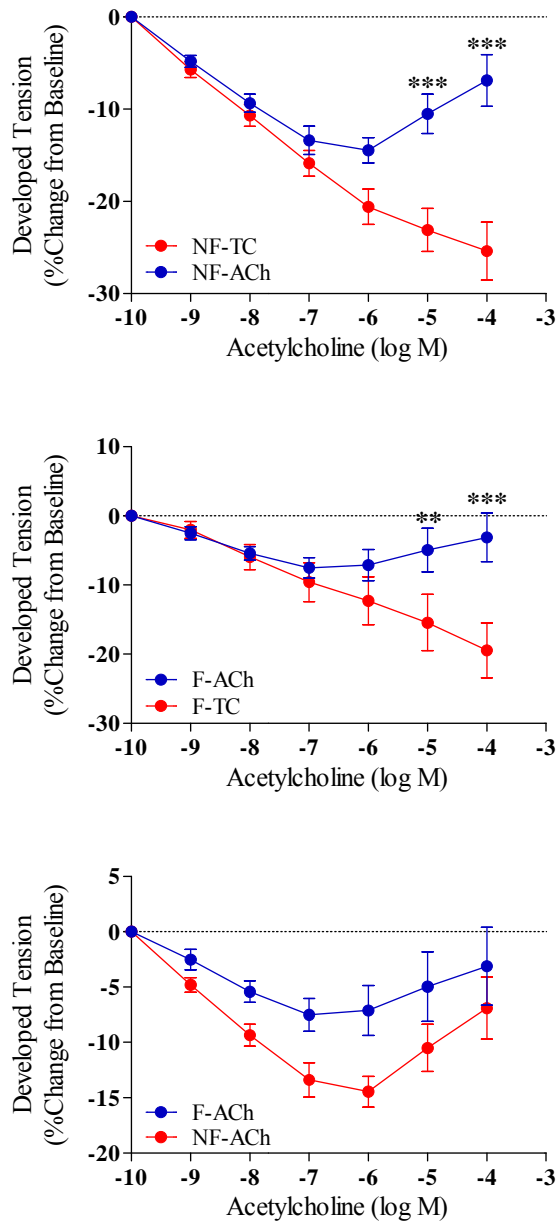


Figure 28. Dose-Response to ACh – Developed Tension (DT) Results. No significant changes were found between NF muscles treated with ACh at lower doses and those serving as time control (TC), however addition of the two highest doses of ACh resulted in a significant recovery in the percent change of DT compared to control [top graph] ($p < 0.001$). No significant changes were found between F muscles treated with ACh at lower doses and those serving as TC, however addition of the two highest doses of ACh resulted in a significant recovery in the percent change of DT compared to control [middle graph] (** $p < 0.01$; *** $p < 0.001$). No significant differences were detected in the percent change of DT in ACh-treated F muscles versus ACh-treated NF muscles [bottom graph].

The results for developed tension (DT) are depicted in **Figure 28**. NF muscles treated with ACh at lower doses (1, 10, and 100 nM and 1 μ M) produced no change in DT compared to time control. When 10 μ M and 100 μ M of ACh were added, treated muscles significantly recovered their percent change in DT compared to time control (10 μ M: -10.50 vs -23.10 ($p < 0.001$); 100 μ M: -6.90 vs -25.35 ($p < 0.001$)). The middle graph shows the same comparison, but with the F tissue group. Again, the two highest doses of ACh showed a significant recovery in DT compared to the time control muscles (10 μ M: -4.96 vs -15.44 ($p < 0.01$); 100 μ M: -3.12 vs -19.45 ($p < 0.001$)), while the four lower doses of ACh produced no change in response compared to control. The response of ACh addition was compared between the two groups of tissue as well. ACh doses elicited the same effect at all six doses in both NF and F muscles, with no significant changes in their DT found.

Time to peak tension (TPT) was the next parameter compared. In **Figure 29**, no significant differences were found between time control and ACh-treated muscles in NF tissue and F tissue. **Figure 29** also shows the comparison of ACh addition in NF tissue versus ACh addition in F tissue. While the NF muscles continue to decrease from baseline upon each dose addition, F muscles preserve their TPT, with values closely mimicking baseline values at all six doses. Here, 1, 10, or 100 nM of ACh did not significantly change the TPT between F and NF muscles. At 1 μ M, F muscles had a percent change in TPT of -0.40 and NF muscles -3.94; a statistically significant change found ($p < 0.05$). Differences were also detected at 10 μ M and 100 μ M ACh-treatments (10 μ M: -0.08 (F) vs -3.39 (NF) ($p < 0.05$); 100 μ M: 0.13 (F) vs -3.90 (NF) ($p < 0.01$)).

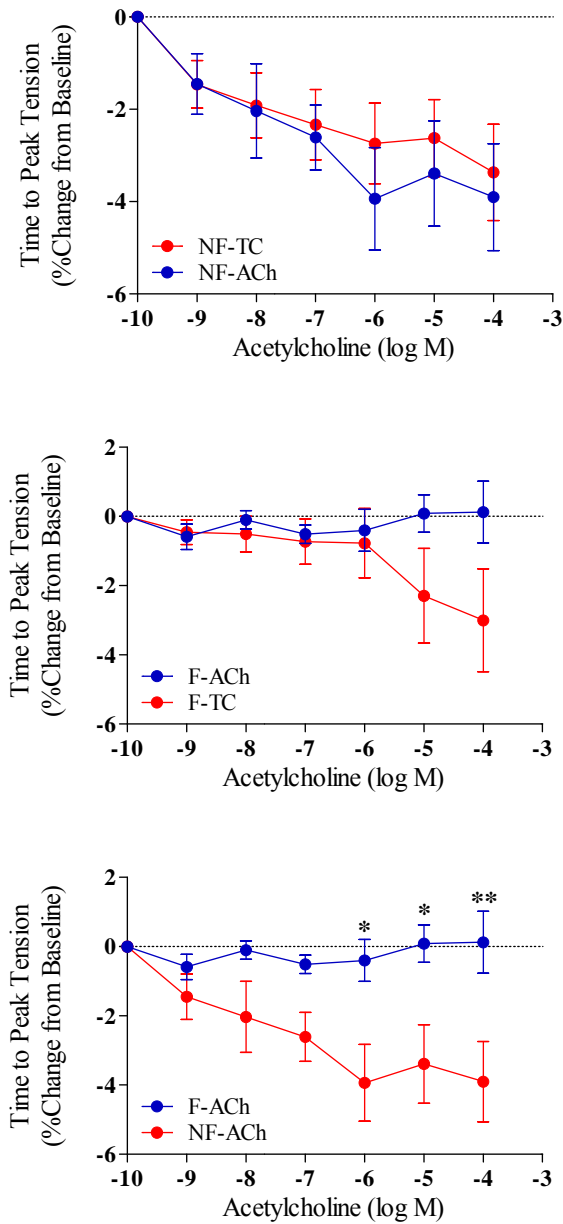


Figure 29. Dose-Response to ACh – Time to Peak Tension (TPT) Results. No significant changes were found between NF muscles treated with ACh and those serving as time control (TC) [top graph]. No significant changes were found between F muscles treated with ACh and those serving as TC [middle graph]. Significant differences were detected in the three highest doses of ACh in F tissue versus NF tissue [bottom graph] (* $p < 0.05$; ** $p < 0.01$).

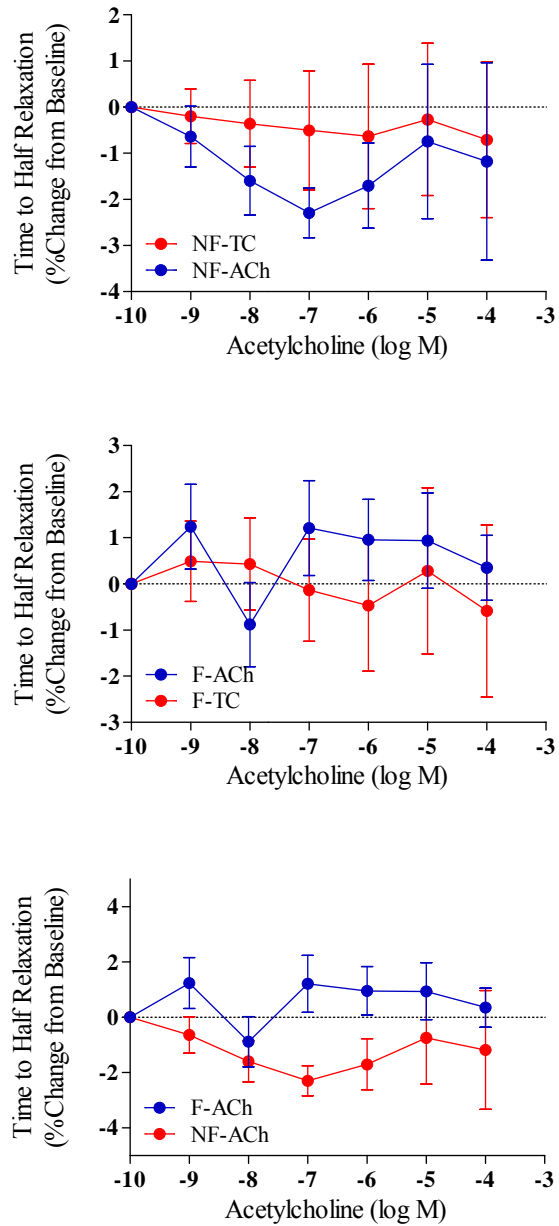


Figure 30. Dose-Response to ACh – Time to Half Relaxation (THR) Results.

No significant changes were found between NF muscles treated with ACh and those serving as time control (TC) [top graph]. No significant changes were found between F muscles treated with ACh and those serving as TC [middle graph]. No significant differences were detected in the percent change of THR in ACh-treated F muscles versus ACh-treated NF muscles [bottom graph].

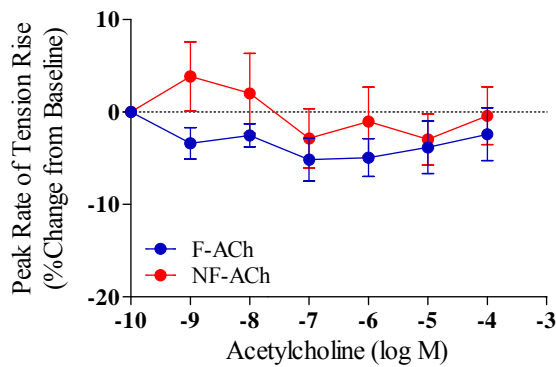
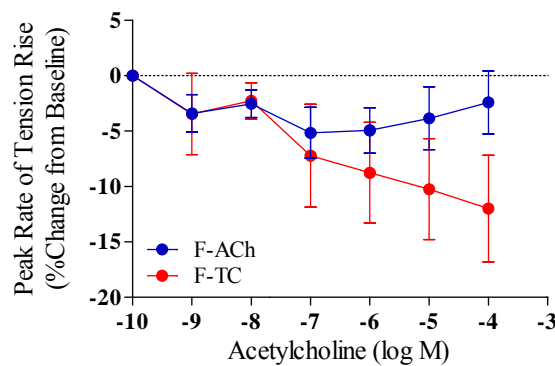
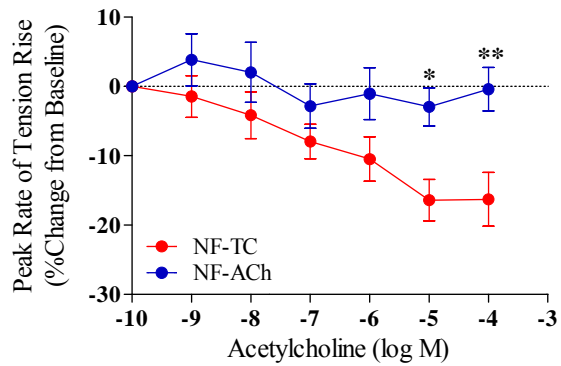


Figure 31. Dose-Response to ACh – Peak Rate of Tension Rise (+dT/dt) Results. Significant differences were found between NF muscles treated with the two highest doses of ACh and those serving as time control (TC) [top graph] (* $p < 0.05$; ** $p < 0.01$). No significant changes were found between F muscles treated with ACh and those serving as TC [middle graph]. No significant differences were detected in the percent change of +dT/dt in ACh-treated F muscles versus ACh-treated NF muscles [bottom graph].

Figure 30 shows the time to half relaxation (THR) results. No significant changes were detected between time control and ACh muscles of NF tissue or time control and ACh muscles of F tissue (shown in **Figure 30a** and **30b**). NF and F tissue, with addition of ACh, did not produce any significant changes at any of the six doses either.

The results of peak rate of tension rise (+dT/dt) were compared in **Figure 31**. In NF tissue, the time control muscles continually decreased in percent with time, while those treated with ACh recovered toward baseline +dT/dt values as the concentration of ACh increased. With the addition of 10 μM ACh, ACh-treated NF muscles had a percent change +dT/dt of -2.96 while time control NF muscles had a percent change +dT/dt of -16.41, a significant change in response ($p < 0.05$). Upon addition of 100 μM ACh, NF muscles had a percent change +dT/dt of -0.40 versus the time control NF muscles of -16.27 ($p < 0.01$). This resulted in a significant increase of +dT/dt with the two most concentrated doses of ACh versus control. The F tissue, depicted in **Figure 31(middle graph)**, trended similarly to the NF tissue, however no significant changes were detected. In comparing the addition of ACh between NF and F tissue, no significant differences were found.

-dT/dt, shown in **Figure 32**, show the same changes as +dT/dt. When comparing NF time control to NF ACh, the two highest doses of ACh resulted in a significant increase in -dT/dt versus control (10 μM : -4.24 (ACh-treated) vs -18.13 (control) ($p < 0.01$); 100 μM : -1.32 (ACh-treated) vs -19.26 (control) ($p < 0.001$). In comparing F time control to F ACh and ACh addition in NF and F tissue, no significant changes occurred in respect to -dT/dt.

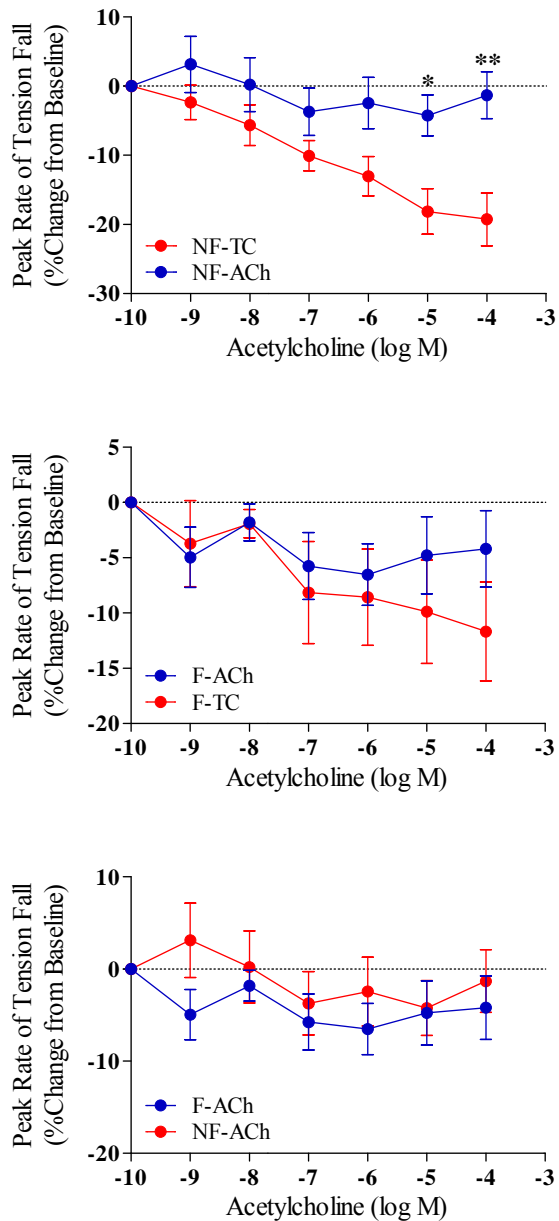


Figure 32. Dose-Response to ACh – Peak Rate of Tension Fall (-dT/dt) Results.

Significant differences were found between NF muscles treated with the two highest doses of ACh and those serving as time control (TC) [top graph] (*p<0.05; **p<0.01). No significant changes were found between F muscles treated with ACh and those serving as TC [middle graph]. No significant differences were detected in the percent change of -dT/dt in ACh-treated F muscles versus ACh-treated NF muscles [bottom graph].

Addition of Isoproterenol (ISO)

One dose of the β -AR agonist ISO was added to both time control and ACh-treated muscles after the ACh dose-response experiments were completed. Results are expressed as the mean percent change from a time immediately before addition of ISO.

The RT results upon addition of ISO are depicted in **Figure 33**. Time control and ACh-treated muscles had significantly different RTs from failing to non-failing groups (TC: -3.9 vs -11.52, $p < 0.001$; ACh: -3.9 vs -9.3, $p < 0.01$). Non-failing muscles had comparable RTs in ACh-treated muscles compared to control (-9.3 vs -11.5) and failing muscles had comparable RTs in ACh-treated versus control groups (-3.9 vs -3.9).

Figure 34 represents DT data collected upon addition of ISO. Time control muscles had a significantly lower percent change in DT in failing versus non-failing tissue (127.5 vs 191.6, $p < 0.01$). ACh-treated muscles also had a significantly lower percent change in DT in failing versus non-failing tissue (47.9 vs 109.8, $p < 0.001$). Looking at the change in non-failing tissue, there was ~43% decrease in DT in ACh-treated muscles compared to control ($(109.8 - 191.6) / 191.6 = 42.7\%$). In failing tissue, there was ~62% decrease in DT in ACh-treated muscles compared to control ($(47.9 - 127.5) / 127.5 = 62.4\%$). Therefore, failing tissue had a greater negative response to DT by approximately 19%.

TPT, depicted in **Figure 35**, significantly changes between sample groups and between drug treatment. There was a significantly greater change in TPT in non-failing muscles than failing muscles for both time control and ACh-treated groups (time control: -36.9 in non-failing; -18.3 in failing) (ACh-treated: -28.0 in non-failing; -12.4 in failing). Looking at non-failing tissue only, there was a significant difference in the percent

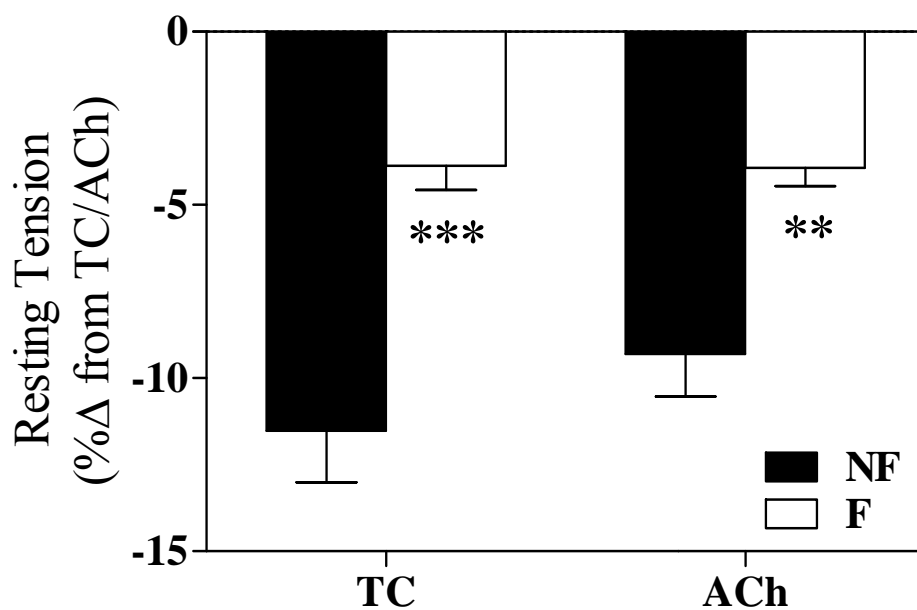


Figure 33. Resting Tension (RT) – Isoproterenol (ISO) Response. Both time control (TC) and ACh-treated muscles had a significantly less percent change in F tissue versus NF tissue after addition of ISO (** p<0.01; *** p<0.001). Addition of ACh had no significant change in the effect of ISO in NF or F groups.

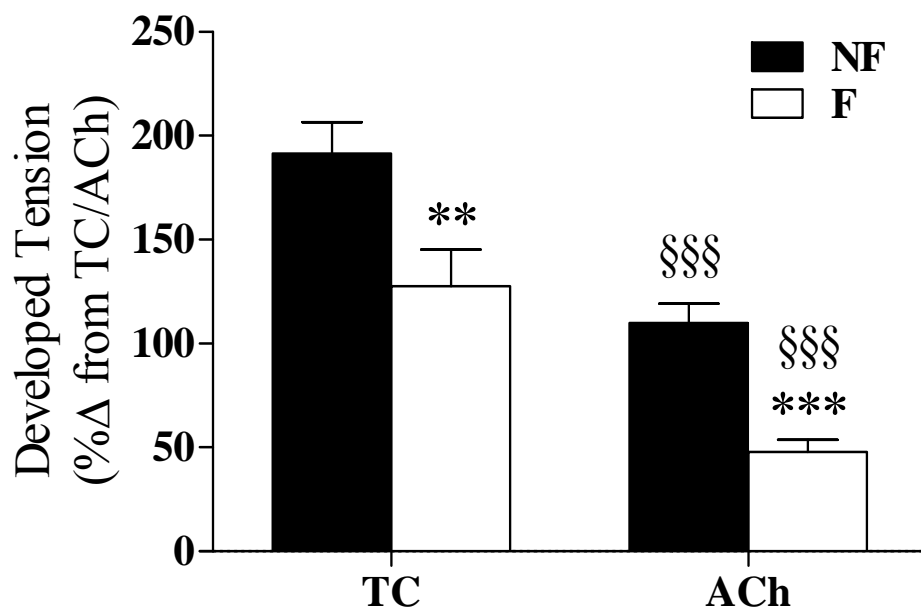


Figure 34. Developed Tension (DT) – Isoproterenol (ISO) Response. Both time control (TC) and ACh-treated muscles had a significantly less percent change in F tissue versus NF tissue after addition of ISO (** p<0.01; *** p<0.001). Addition of ACh significantly decreased the percent change in DT in NF tissue (43% decrease) and F tissue (62% decrease) compared to muscles only treated with ISO (§§§ p<0.001).

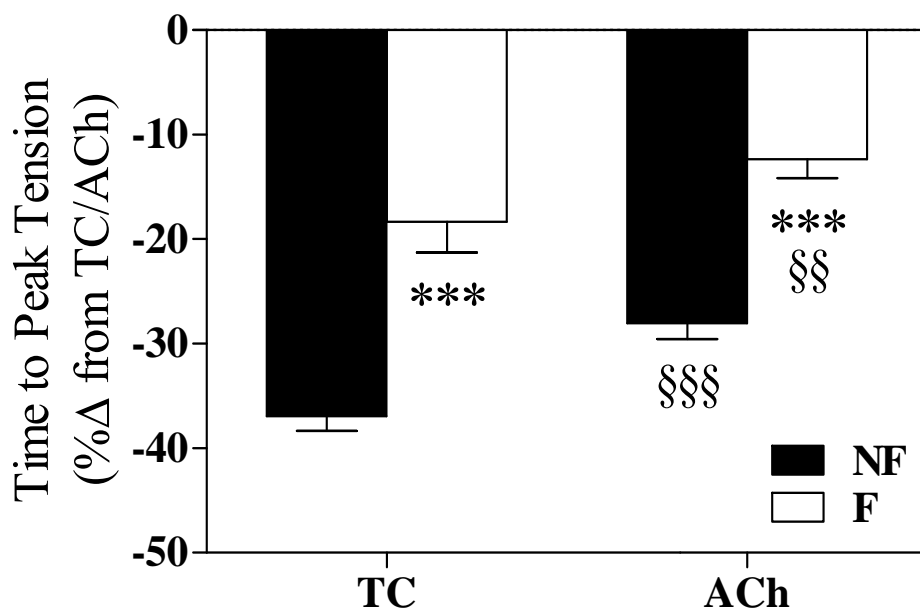


Figure 35. Time to Peak Tension (TPT) – Isoproterenol (ISO) Response. Both time control (TC) and ACh-treated muscles had a significantly less percent change in F tissue versus NF tissue after addition of ISO (** $p < 0.001$). Addition of ACh significantly decreased the percent change in TPT in NF tissue and F tissue compared to muscles only treated with ISO (§§§ $p < 0.001$; §§ $p < 0.01$).

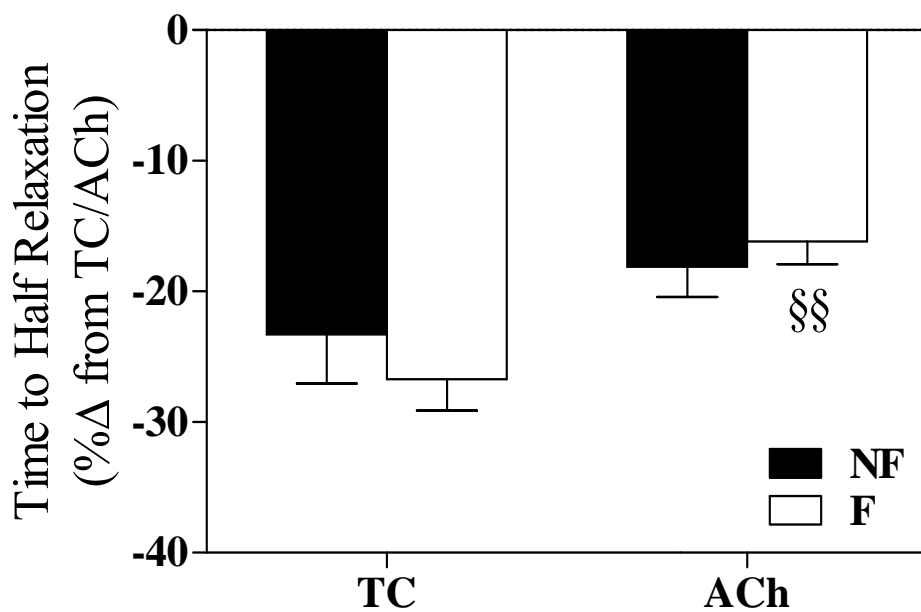


Figure 36. Time to Half Relaxation (THR) – Isoproterenol (ISO) Response. Time control (TC) and ACh-treated muscles had no significant percent change in F tissue versus NF tissue after addition of ISO. Addition of ACh significantly decreased the percent change in THR in F tissue compared to muscles only treated only with ISO (^{§§} p<0.01). Addition of ACh did not significantly change in THR in NF tissue versus TC.

change of TPT from ACh-treated muscles versus time control (-28.0 vs -36.9). Also, the percent change in TPT was significantly different in failing versus non-failing tissue (-12.4 vs -18.3).

The next contractile parameter analyzed was THR. As shown in **Figure 36**, THR in time control muscles did not significantly change in failing tissue versus control (-26.7 vs -23.3). ACh-treated muscles also did not significantly change in failing versus non-failing muscles (-16.2 vs -18.1). THR was comparable in non-failing and ACh-treated muscles (-23.3 and -18.1) while THR in failing muscles was significantly different in ACh-treated versus time control muscles (-16.2 vs -26.7).

+dT/dt, in **Figure 37**, did not significantly change when comparing ACh-treated muscles in failing versus non-failing groups (37.5 vs 116.7). There was a significant percent change in +dT/dt in time control muscles comparing failing to non-failing tissue (112.0 vs 253.7, $p < 0.001$). Both non-failing and failing muscles did significantly change in +dT/dt when comparing ACh-treated to time control muscles (non-failing: 116.7 vs 253.7, $p < 0.001$; failing: 37.5 vs 112.0, $p < 0.05$).

-dT/dt, shown in **Figure 38**, did not significantly change when comparing ACh-treated muscles in failing versus non-failing groups (37.2 vs 94.6). There was a significant percent change in -dT/dt in time control muscles comparing failing and non-failing tissue (114.2 vs 215.3, $p < 0.01$). Both non-failing and failing muscles did significantly change in -dT/dt when comparing ACh-treated to time control muscles (non-failing: 94.6 vs 215.3, $p < 0.001$; failing: 37.2 vs 114.2, $p < 0.05$).

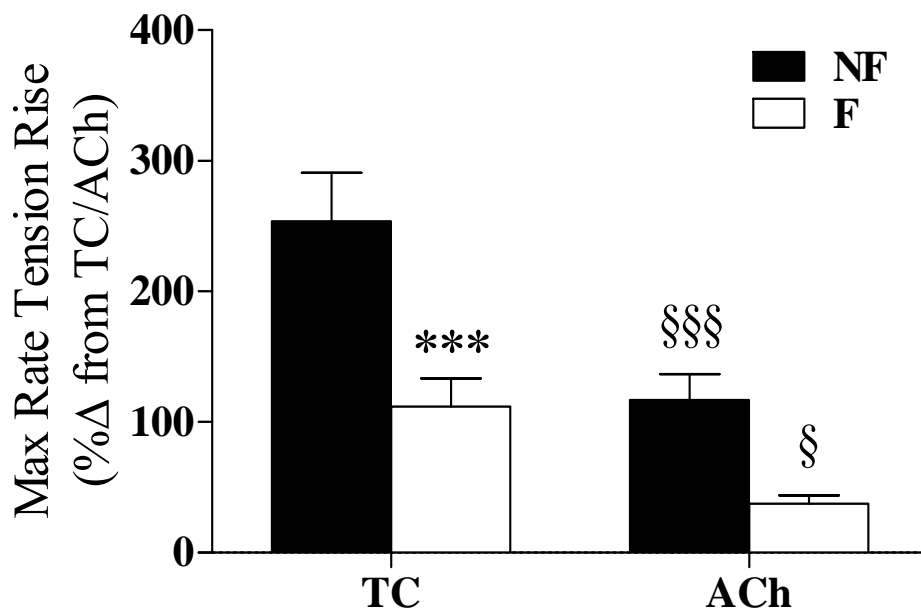


Figure 37. Peak Rate of Tension Rise (+dT/dt) – Isoproterenol (ISO) Response. Time control (TC) muscles had significantly less of a response in F tissue versus NF tissue to ISO (***) p<0.001). Addition of ACh significantly decreased the +dT/dt in F and NF muscles versus their respective TC group (§§§ p<0.001; § p<0.05).

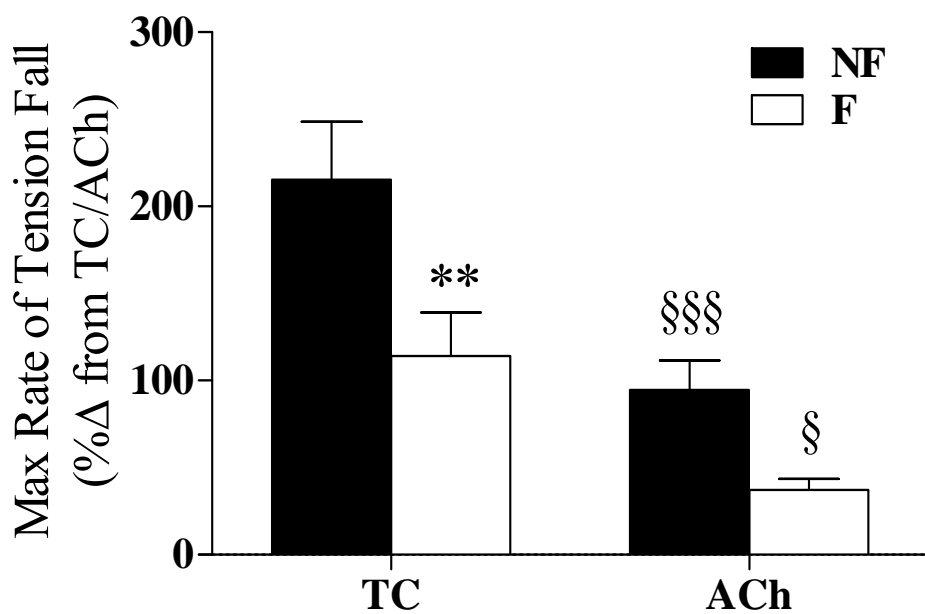


Figure 38. Peak Rate of Tension Fall (-dT/dt) – Isoproterenol (ISO) Response. Time control (TC) muscles had significantly less of a response in F tissue versus NF tissue to ISO (** p<0.01). Addition of ACh significantly decreased the -dT/dt in F and NF muscles versus their respective TC group (§§§§ p<0.001; § p<0.05).

CHAPTER IV

DISCUSSION

4.1 Effect of Total Muscarinic Receptor Density and Affinity in Failure and Upon LVAD Support

ANS imbalance is a characteristic in HF. The SNS has been the focus of research for the past 20+ years, resulting in definitive conclusions about its role in failure. With the consensus that the SNS is overactivated in HF, leading to a significant downregulation of β -ARs, new drug therapies targeting β -ARs were introduced. Research on the PNS in HF has led to conflicting results, allowing for no consensus to be reached and potential therapies targeting the PNS disregarded. Muscarinic receptor densities have been studied in various models of HF, however inconsistent findings have led to more confusion and less conclusions about the PNS in HF.

Some early studies of muscarinic receptors report a significant decrease in receptor density in failure. Vatner et al in 1988 used left ventricular sarcolemma from mongrel canines to measure muscarinic receptor densities. With control (n=10) and HF (n=8)

they found densities to be significantly reduced (3.6 ± 0.4 versus 5.6 ± 0.6 pmol/mg, $p < 0.05$) in the canine model of HF⁵⁶. Mertens et al used rat left ventricular tissue (n=6 per group) to determine a significant decrease in muscarinic receptor density compared to control (221.0 ± 8.9 versus 308.8 ± 16.1 fmol/mg, $p < 0.05$)³⁷.

The first human studies on muscarinic receptor densities found no significant changes between non-failing and failing tissue. Bohm and colleagues used 16 patients with DCM and coronary artery disease (CAD), aged between 21-59 years, against 5 controls (22-31 years old). They found no significant change in receptor density (275 ± 21 versus 211 ± 22 fmol/mg in failure)³. A review in 1999 by Giessler and others highlighted the work done on muscarinic receptors up to that time. Their own research examined muscarinic receptor density in right atrium and left ventricle tissue. The densities did go up in HF (n=11) compared to control (n=5) but not enough to be statistically significant. It is important to point out that in this case, 5 control hearts came from patients with a mean age of 33 years old while the 11 HF patients had a mean age of 51 years old¹⁹.

Coinciding with our current findings, researchers in France used positron emission tomography (PET) to find a significant upregulation of muscarinic receptor density in HF patients (n=20) compared to control (n=12) ($p < 0.005$)³². Wilkinson and colleagues examined atrial and ventricular muscarinic receptor densities in a canine model of HF. No significant differences in density were found in the atrium but a significant increase in muscarinic receptor density was found in the left ventricular HF model. Using n=4 (HF) versus n=6 (control), they found densities to be 245.0 ± 25.0 fmol/mg protein in failure compared to 160.0 ± 10.0 fmol/mg in control ($p < 0.01$)⁶⁰. Vatner et al also found a

significant increase in muscarinic receptors in the pacing model of HF. Canines with HF were found to have densities 153.0 ± 6.2 fmol/mg versus 124.0 ± 7.4 fmol/mg in control. Vatner et al had previously found a significant decrease in muscarinic receptor density in a canine model of HF (induced by aortic banding) and stated that differences found between these experiments were due to differing models of HF⁵⁷.

This current study was aimed to clarify the conflicting results generated by the past twenty years of research on muscarinic receptors in relation to HF. Several differences from previous studies to this current study include the model being tested, age, and sample size. Model differences may factor in differing results because muscarinic receptor densities may be different among species. Also, animal models do not form HF over a prolonged, natural time course. The difference in disease acquisition may add to conflicting muscarinic receptor density findings. Age is also an important factor in choosing a sample population, especially when measuring muscarinic receptors. It is established that muscarinic receptor density is significantly decreased as age increases, therefore, studies with large differences in age may not appropriately represent muscarinic receptor density⁶. Finally, sample sizes may contribute to differing conclusions. With a small sample size, such as five, differences in density are more difficult to detect.

With a large sample selection of human hearts from patients with a similar mean age, this study found total muscarinic receptor density to be significantly upregulated in the failing heart (275.8 ± 11.9 vs 194.1 ± 17.3 fmol/mg ($p < 0.01$)) and even more significantly upregulated upon LVAD support compared to control (315.8 ± 11.9 ,

p<0.001). A significant increase in receptor density may be opposing β -AR stimulation by inhibiting the adenylyl cyclase, cAMP pathway that is overactivated in the failing human heart. Because M_2 receptors are predominant, and they act by inhibiting this pathway, an increase in density may be a mechanism for reducing sympathetic overstimulation. Upon LVAD support, muscarinic receptors remain upregulated compared to control. β -AR densities recover with LVAD support, having densities after an LVAD mimicking non-failing values, therefore, our findings on tissue with LVAD support are surprising⁴². Although the reason why muscarinic receptor densities remain upregulated in LVAD remains unknown, one could speculate that it is in response to an increase in β -AR density.

An upregulation of muscarinic receptor density in failure is clear, and is further supported by previous studies that found Gi protein, that which couples $M_{2/4}$ receptors, also upregulated in failure^{2,17,57}. This increase in Gi provides evidence that the effects regulated by M_2/M_4 receptors are increased in HF². $M_{2/4}$ receptors inhibit AC, cAMP pathway using Gi only when the pathway is turned on by the SNS. During failure, the PNS may act to increase opposition of established SNS overstimulation by increasing the amount of muscarinic receptors. More muscarinic receptors coupled to Gi would be able to inhibit the overactivated SNS.

PNS activity on the heart is regulated at various levels, therefore muscarinic receptor density and Gi protein levels alone cannot be the answer to PNS control on the heart. Although muscarinic receptors act as the target of the PNS on cardiomyocytes, the vagus nerve is an important regulator of the PNS and is found to have diminished control in

HF⁶¹. Recent studies have found vagal nerve stimulation to increase survival and improve autonomic balance in animal models of HF⁶¹. No current study has performed vagal nerve stimulation and then measured muscarinic receptor density on cardiomyocytes, although it would be interesting to see if stimulation of the vagus nerve produces changes on receptor density.

When looking at antagonist affinity to muscarinic receptors, this current study found no significant change in affinity between NF and F groups. However, a significant loss in affinity was found in F+LVAD versus control. Our findings in NF and F human hearts were in agreement to other studies that found no change in affinity between groups^{3,32,56,57}. To our knowledge, this is the first study to measure muscarinic receptors upon LVAD support, therefore the only study to find changes in affinity. LVADs have been shown to recover remodeling in the failing heart, including restoring β -AR density to NF values. A possible reason the antagonist affinity decreases upon LVAD support may be because a significant increase in receptor stimulation is no longer necessary. Receptors may conformationally change or desensitize in response to SNS regulation.

4.2 Muscarinic Subtypes in the Non-failing, Failing, and LVAD Human Hearts

The functional role of muscarinic receptor subtypes was not realized until the 1990s⁵⁸. In the heart, M₂ was accepted as the only functional subtype until studies on rats, chicks, canines, and other species found non-M₂ subtypes existing^{52,58}. The first human study to detect multiple muscarinic receptor subtypes in the heart was published in 2001⁵⁸.

In this current study, we were able to support the idea that there are multiple muscarinic receptor subtypes in the NF, F, and F + LVAD support human heart. Using non-labeled subtype selective antagonists at established K_i concentrations, we were able to fraction subtypes in our three sample populations. Because each heart resulted in a percent binding over 100%, we chose to interpret the raw data and to normalize the data to 100%.

When looking at the raw data, we found no significant change in the percent of M_1 , M_2 , or M_4 between NF, F, and F+LVAD. The percent of M_3 significantly decreased in failure compared to control and significantly increased back up to NF results upon LVAD support. When looking at the normalized data, we found no significant change in the percent of M_1 or M_4 between NF, F, and F+LVAD groups. The same change in the percent of M_3 was found once normalized, significantly decreasing in failure compared to control and significantly increasing back to NF results upon LVAD support. The one difference between the normalized and raw data was with the percent of M_2 . When comparing NF to F groups, the percents did not significantly change in either representation of the data. However, once normalized there was found to be a significant decrease in the percent of M_2 upon LVAD support compared to control, a difference not detected in the raw data.

The percents of M_1 , M_2 , and M_4 did not change significantly between the groups tested, although a change in receptor density should not be disregarded. We do not know how the densities of each subtype change in response to failure or LVAD support, however with data we have found, we can speculate about how the subtypes may change

in density. For example, we know total muscarinic receptor density is upregulated both in F and F+LVAD support compared to NF tissue. We may speculate that the predominant subtypes, M₂ and M₄, which are also the receptors coupled to the inhibitory Gi protein, increase in density while the density of M₁ and M₃ stay the same, respectively. This speculation could result in the percent of M₂ and M₄ staying the same, with a slight decrease in the percent of M₁ and M₃ (significant enough for M₃ because the percent in the left ventricle is only a small fraction of the whole). This is one possible mechanism to explain total density increasing with percents changing as described above, although other mechanisms are also possible.

Our study was the first to measure the percent of muscarinic subtypes in NF, F, and F+LVAD tissue; however researchers have examined the idea of multiple subtypes existing in the non-diseased human heart. Huizen Wang and colleagues used multiple experimental techniques to detect muscarinic receptor subtypes. They performed competition binding studies using pirenzepine, methoctramine, 4-DAMP, and tropicamide to detect the percent binding of antagonists to receptor subtypes. Their data found (in %) 30.3 ± 10.4 using pirenzepine, 78.2 ± 9.8 with methoctramine, 15.4 ± 2.5 for 4-DAMP, and 18.7 ± 8.4 using tropicamide. Unlike our current study, Wang et al performed competition binding studies with varying doses of each non-labeled subtype selective antagonist, while we kept the antagonist concentration constant and varied the time of incubation. By varying the concentration of selective antagonists, they were able to yield pK_i values. Using previous literature and established pK_i values for each subtype binding to antagonists, these researchers concluded that pirenzepine was binding

to M₁ receptors, methoctramine to M₂, 4-DAMP to both M₃ and M₁, and tropicamide to M₃ and M₂. Therefore, they detected the presence of M₁, M₂, and M₃ receptors using competition binding experiments. They also used reverse-transcriptase polymerase chain reaction (RT-PCR), Western blotting, and confocal microscopy to examine the muscarinic receptor subtypes. Results from Western blotting and confocal microscopy supported the presence of M₁, M₂, M₃, and M₅ subtypes. Neither technique was able to detect M₄. RT-PCR, on the other hand, detected the presence of mRNA for all five subtypes⁵⁸.

More recently, Perez and others examined the existence of non-M₂ subtypes in the human heart using immunoblotting, ELISA, and RT-PCR. All three experimental techniques supported the idea that all 5 muscarinic receptor subtypes are present in human atrial and ventricular tissue. They further suggest that these subtypes are able to act as non-interacting monomers and interacting oligomers⁴⁶.

With multiple subtypes existing in the human heart, multiple signaling pathways and elicited responses must be present. In the ventricles, M₂ and M₄ subtypes couple to the inhibitory G_i protein. Upon activation, G_i inhibits adenylyl cyclase which decreases levels of cAMP and PKA activity. This effects Ca⁺⁺-cycling proteins on the SR, producing a negative chronotropic and inotropic effect on the heart. M₁, M₃, and M₅ activate stimulatory pathways and are coupled to G_q proteins. Upon activation, PLC is stimulated which cleaves phosphatidylinositol bisphosphate (PIP₂) into IP₃ and DAG. Recently, Kitazawa et al used mice atria to demonstrate a positive inotropic response upon activation of M₃.

4.3 Muscle Function

Muscle function experiments were performed to see if a relationship existed between total muscarinic receptor density differences in non-failing and failing hearts and the functional response of cardiac muscle. We speculated that, because a significant increase in muscarinic receptor density exists in failing tissue, the negative inotropic and chronotropic effects on the heart would be greater in failure.

Baseline parameters were measured to ensure that differences found in the six contractile parameters were due to drug responses and not to initial differences in muscle function. As shown in Table III, failing tissue was found to have significantly decreased developed tension (DT), time to peak tension (TPT), and time to half relaxation (THR) than the non-failing groups. This phenomenon has been shown in previous work, indicating that failing tissue is weaker than healthy, non-diseased hearts. Because of differences in the contractile function of tissue groups, data was represented as a percent change from baseline. Muscles within each group were also analyzed at baseline. Table IV shows that time control and ACh-treated muscles began at comparable contractile measurements in both non-failing and failing groups.

Looking at the resting tension (RT) contractile parameter upon addition of ACh doses, this parameter does not significantly change between non-failing and failing muscles treated with ACh, or when comparing non-failing time control and ACh muscles, and failing time control and ACh-treated muscles (shown in Figure 24). RT is the amount of tension generated while the muscle is not contracting. Because RT does not require stimulation of contraction or is in response to muscarinic stimulation, this lack of changes

found is not surprising. These results do demonstrate the loss in RT, with or without ACh-treatment – as a result of time.

Developed tension (DT) is one of the most important of the six contractile parameters measured because it is the tension produced from a muscle's resting state to the highest point of contraction. DT is a direct measure of muscle function and how well the muscle is contracting. As shown in Figure 25, lower doses of ACh produce no change in DT compared to control. However, when higher doses of ACh were added, DT recovered compared to control in both non-failing and failing tissue. Because this dose-response curve was in the absence of β -AR stimulation, higher doses of ACh could be stimulating the less predominant muscarinic receptor pathway ($M_1/M_3/M_5$). If this were true, these muscarinic receptors would stimulate Ca^{++} movement within cells, causing a positive response to ACh. It is important to note that, although the two highest doses of ACh elicit recovery in DT in both groups, their response is still negative compared to baseline measures. If these higher doses were added initially, they may or may not have produced a positive response on DT. Also, when looking at ACh-treated muscles in failing versus non-failing tissue, no statistically significant differences were found. Therefore, ACh without stimulation of β -AR signaling did not change how well the muscle was contracting in failing hearts versus non-failing hearts.

One of the timing parameters, time to peak tension (TPT), did not show significant differences when comparing time control and ACh-treated muscles in each group. The percent change from baseline declined as time increased in both time control and ACh-treated muscles in the healthy heart. Failing tissue did not decline as great as non-failing

tissue, yet time control and ACh muscles produced the same effect. When comparing ACh addition in failing to non-failing muscles, TPT significantly recovered to baseline in failing tissue while non-failing tissue continued to decline as ACh doses increased.

Another timing parameter, time to half relaxation (THR), showed no changes between muscle types or between non-failing and failing ACh-treated muscles. However, a high amount of variability may restrict differences from being found.

The peak rate of tension rise ($+dT/dt$) is the point where the muscle is contracting the fastest and the peak rate of tension fall ($-dT/dt$) is the point where the muscle is relaxing the fastest. Neither of these parameters changed in time control or ACh-treated failing muscles nor did they differ when comparing failing ACh-treated muscles to non-failing ACh-treated muscles. For both of these parameters, non-failing muscles treated with ACh at higher doses showed significant recovery compared to the non-failing time control muscles.

Adding ISO to all of the muscles at the end of the experiment allowed us to see the affect ACh had on muscles with sympathetic stimulation. Most of the contractile parameters (all except for THR) elicited changes between failing and non-failing tissue, a response due to the difference in tissue type. ACh-treated muscles also produced different responses compared to their time control counterparts in five of the six contractile parameters (all except for RT).

Landzberg and colleagues examined left ventricular contractility in six normal patients and seven patients 1-3 years after cardiac transplantation. In this study, patients were infused with dobutamine, ACh, atropine, dobutamine + ACh, and dobutamine + atropine.

Left ventricular +dP/dt was measured five minutes after each infusion and after addition of a control (5% dextrose in water). Results show that left ventricular +dP/dt significantly increases with addition of the β -AR agonist dobutamine. ACh, the cholinergic agonist, alone did not produce a change in +dP/dt compared to control. When ACh was infused with dobutamine, a small increase in +dP/dt was found. This work shows that muscarinic stimulation or blockade modulates sympathetic activity, demonstrating the important interactions of the SNS and PNS to regulate functional responses of the heart³⁰.

Another study, by Du et al, examined the effects of ACh and ACh with noradrenaline on human right atrial and left ventricular trabeculae from 61 donor hearts. Similar to our findings, results from this experiment indicated that ACh elicited an increase in ventricular contractility at high doses. However, when ACh was added after pre-stimulation with noradrenaline, ACh decreased contractility. They also showed that atropine blocked the positive inotropic response elicited by ACh alone and that these responses did not change when propranolol was introduced¹⁵.

4.4 Summary

Total muscarinic receptor densities are upregulated in human HF. This result could be in response to overactivated sympathetic stimulation. Because the inhibitory muscarinic receptors, which take up approximately 80% of the total number of receptors, inhibit the β -AR stimulated pathway, an increase in muscarinic receptors may be a compensatory mechanism to antagonize the effects of the overstimulated SNS seen in HF. This theory

is supported by previous studies that found a significant increase in Gi protein, that which couples M₂ and M₄, in human HF². In failing hearts with LVAD support, muscarinic receptor densities remain significantly upregulated versus control, instead of showing recovery to NF densities like β -ARs do upon LVAD support. This may or may not be due to receptor subtype changes.

Muscarinic receptor subtypes differ in the G protein they couple, causing activation of different signaling pathways. Even-numbered receptors couple Gi and produce a negative inotropic and chronotropic effect while odd-numbered receptors couple to Gq and produce a positive inotropic and chronotropic effect. Because multiple muscarinic receptor subtypes exist that elicit opposite responses on the heart, the total density differences found between groups may be a result of one, a few, or all subtype densities changing. With the differences found in the percent of each subtype in the various tissue, speculations may be made concerning the density differences of subtypes in each sample group. Upon LVAD support, SNS balance has been found to be restored⁴². With inhibitory receptor subtypes no longer needed in increased abundance, stimulatory receptors may be synthesized more to increase their fraction of total muscarinic receptors acting on cardiac myocytes.

The goal in investigating muscle function on NF and F tissue was to see if a relationship existed between the functional response of fresh cardiac muscles and the changes found in muscarinic receptor densities. In the dose-response curves, a significant recovery was found when comparing higher doses of ACh to control muscles in both NF and F tissue types (DT, TPT, +dT/dt, and -dT/dt results). With a lack of β -AR

stimulation, M₂ and M₄ receptor pathways may only be signaling constitutively. M₁, M₃, and M₅, with high concentrations of a ligand, elicit a positive response on contractility – resulting in the recovery seen in four of the contractile parameters. Once ISO is added, M₂ and M₄ receptors are able to activate Gi and inhibit the AC-cAMP-PKA signaling pathway to produce an inhibitory response. This is shown in DT, TPT, THR, +dT/dt, and –dT/dt contractile parameters.

Through the radioligand binding assays, competition binding assays, and muscle function analysis, it was shown that HF is associated with a significant increase in total muscarinic receptor density, which remains upregulated with LVAD support. The percent of M₁-M₄ receptor subtypes differed in the patient populations as well, showing that muscarinic receptors play both an inhibitory and stimulatory role on heart rate and force of contraction. The muscle function data supported the increase in total muscarinic receptor densities relating to greater decreases in muscle contractility measures. In conclusion, it is known that the overactivated SNS is a target of therapy in human HF – which was found through years of research on its activity and signaling. β-ARs are a target of medications that block the receptor from activating a stimulatory signaling pathway. With findings from this current study and others, the role of the PNS may be further investigated as a target for novel therapeutic approaches in tackling human HF.

REFERENCES

1. Bibeovski, S. and Dunlap, M. E. (2004). Prevention of diminished parasympathetic control of the heart in experimental heart failure. *American Journal of Physiology*. 287; H1780-H1785.
2. Bohm, M., Gierschik, P., Jakobs, K.H., Pieske, B., Schnabel, P., Ungerer, M., and Erdmann, E. (1990). Increase of Gi alpha in human hearts with dilated but not ischemic cardiomyopathy. *Circulation*. 82; 1249-1265.
3. Bohm, M., Ungerer, M., and Erdmann, E. (1990). Beta adrenoceptors and m-cholinoceptors in myocardium of hearts with coronary artery disease or idiopathic dilated cardiomyopathy removed at cardiac transplantation. *American Journal of Cardiology*. 66; 880-882.
4. Bristow, M.R. (2000). Beta-adrenergic receptor blockade in chronic heart failure. *Circulation*. 101; 558-569.
5. Brodde, O.E., and Michel, M. C. (1999). Adrenergic and muscarinic receptors in the human heart. *Pharmacological Reviews*. 651-675.
6. Brodde, O.E., Kanschak, U., Becker, K., Ruter, F., Poller, U., Jakubetz, J., Radke, J., and Zerkowski, H.R. (1998). Cardiac muscarinic receptors decrease with age. In vitro and in vivo studies. *Journal of Clinical Investigation*. 2; 471-478.
7. Cappola, T. P. (2008). Molecular remodeling in human heart failure. *Journal of the American College of Cardiology*. 137-138.
8. Caulfield, M. P. (1993). Muscarinic receptors: Characterization, coupling and function. *Pharmacology and Therapeutics*. 58; 319-379.
9. Cohen-Armon, M., Schreiber, G., and Sokolovsky, M. (1984). Interaction of the antiarrhythmic drug amiodarone with the muscarinic receptor in rat heart and brain. *Journal of Cardiovascular Pharmacology*. 6; 1148-1155.
10. Colucci, W.S. (1997). Molecular and cellular mechanisms of myocardial failure. *American Journal of Cardiology*. 80; 15L-25L.
11. Cox, E.A. and Kwatra, M.M. (2007). Inhibition of 3H-QNB binding to subtypes of muscarinic acetylcholine receptors by amiodarone. *Anesthesiology*. 107; A1848.

12. Cullen, M.E., Yuen, A.H., Felkin, L.E., et al. (2006). Myocardial expression of the arginine:glycine amidinotransferase gene is elevated in heart failure and normalized after recovery: potential implications for local creatine synthesis. *Circulation*. 114; 116-20.
13. DiPaola, N.R., Sweet, W.E., Stull, L.B., Francis, G.S., and Moravec, C.S. (2001). Beta-adrenergic receptors and calcium cycling proteins in non-failing, hypertrophied, and failing human hearts: transition from hypertrophy to failure. *Journal of Molecular and Cellular Cardiology*. 33; 1283-1295.
14. DiPaola, N.R., Mattiello, J.A., Jeevanandam, V., Houser, S.R., Margulies, K.B. (1998). Myocyte recovery after mechanical circulatory support in humans with end-stage heart failure. *Circulation*. 97; 2316-2322.
15. Du, X.Y., Schoemaker, R.G., Bos, E., and Saxena, P.R. (1995). Characterization of the positive and negative inotropic effects of acetylcholine in the human myocardium. *European Journal of Pharmacology*. 284; 119-127.
16. Felder, C. C. (1995). Muscarinic acetylcholine receptors: signal transduction through multiple effectors. *The FASEB Journal*. 9; 619-625.
17. Feldman, A., Cates, A., Bristow, M., Van Dop, C. (1989). Altered expression of the alpha-subunit of G proteins in failing human heart. *Journal of Molecular and Cellular Cardiology*. 21; 359-365.
18. Feldman, D. S., Carnes, C. A., Abraham, W. T., and Bristow, M. R. (2005). Mechanisms of disease: β -adrenergic receptors – alterations in signal transduction and pharmacogenomics in heart failure. *Nature*. 2; 475-483.
19. Giessler, C., Dhein, S., Ponicke, K., and Brodde, O. (1999). Muscarinic receptors in the Failing human heart. *European Journal of Pharmacology*. 375; 197-202.
20. Hall, J.L, Fermin, D.R., Birks, E.J., Barton, P.J.R., Slaughter, M., Eckman, P., Baba, H.A., Wohlschlaeger, J., and Miller, L.W. (2011). Clinical, molecular, and genomic changes in response to a left ventricular assist device. *Journal of the American College of Cardiology*. 57; 641-652.
21. Heart Failure. *American Heart Association*. Retrieved August 2009 from <http://www.americanheart.org/presenter.jhtml?identifier=1486>.
22. Hellgren, I., Mustafa, A., Riazi, M., Suliman, I., Sylven, C., and Adem, A. (2000). Muscarinic M3 receptor subtype gene expression in the human heart. *Cellular and Molecular Life Sciences*. 57; 175-180.

23. Houser, S.R., Piacentine, V., and Weisser, J. (2000). Abnormalities of calcium cycling in the hypertrophied and failing heart. *Journal of Molecular and Cellular Cardiology*. 32; 1595-1607.
24. Jaski, B.E., Jessup, M.L., Mancini, D.M., Cappola, T.P., Pauly, D.F., Greenberg, B., Borow, K., Dittrich, H., Zsebo, K.M., and Hajjar, R.J. (2009). Calcium upregulation by percutaneous administration of gene therapy in cardiac disease (CUPID trial), a first-in-human phase ½ clinical trial. *Journal of Cardiac Failure*. 15; 171-181.
25. Katz, A.M. (1992). *Physiology of the Heart*. 2nd Edition. Raven Press, Ltd.
26. Keys, J. R. and Koch, W. J. (2004). The adrenergic pathway and heart failure. *Recent Progress in Hormone Research*. 59; 13-30.
27. Kroeze, W. K., Sheffler, D. J., and Roth, B. L. (2003). G-protein-coupled receptors at a glance. *Journal of Cell Science*. 116;4867-4869.
28. Kuhn, M., Voss, M., Mitko, D, et al. (2004). Left ventricular assist device support reverses altered cardiac expression and function of natriuretic peptides and receptors in end-stage heart failure. *Cardiovascular Research*. 64; 308-314.
29. Lahiri, M. K, Kannankeril, P. J., and Goldberger, J. J. (2008). Assessment of autonomic function in cardiovascular disease. *Journal of the American college of Cardiology*. 51; 1725-1733.
30. Landzberg, J.S., Parker, J.D., Gauthier, D.F., and Colucci, W.S. (1994). Effects of intracoronary acetylcholine and atropine on basal and dobutamine-stimulated left ventricular contractility. *Circulation*. 89; 164-168.
31. Left Ventricular Assist Device. *American Heart Association*. Retrieved July 2009 from <http://www.americanheart.org/presenter.jhtml?identifier=4599>.
32. LeGuludec, D., Cohen-Solal, A., Delforge, J., Delahaye, N., Syrota, A., and Merlet, P. (1997). Increased myocardial muscarinic receptor density in idiopathic dilated cardiomyopathy. *Circulation*. 96; 3416-3422.
33. Li, M., Zheng, C., Sato, T., Kawada, T., Sugimachi, M., and Sunagawa, K. (2004). Vagal nerve stimulation markedly improves long-term survival after chronic heart failure in rats. *Circulation*. 109; 120-124.
34. Lloyd-Jones, D., Adams R.J., Brown, T.M., et al. (2010). Heart disease and stroke statistics – 2010 update. A report from the AHA statistics committee and stroke statistics subcommittee. *Circulation*. 121; e1-e170.

35. Lympelopoulos, A., Rengol, G., Funakoshi, H., Eckhart, A. D., and Koch, W. J. (2007). Adrenal GRK2 upregulation mediates sympathetic overdrive in heart failure. *Nature*. 13; 315-323.
36. Medline Plus: Heart Failure. *U.S. National Library of Medicine and The National Institute of Health*. Retrieved July 2009 from www.nlm.nih.gov/medlineplus/heartfailure.html.
37. Mertens, M.J.F., Batink, H.D., Mathy, M-J., Pfaffendorf, M., and van Zwieten, P.A. (1995). Reduced muscarinic cholinceptor density and sensitivity in various models of experimental cardiac hypertrophy. *Journal of Autonomic Pharmacology*. 15; 465-474.
38. Mirro, M.J., Manalan, A.S., Bailey, J.C., and Watanabe, A.M. (1980). Anticholinergic effects of disopyramide and quinidine on guinea pig myocardium. *Circulation Research*. 47; 855-865.
39. Mori, K., Hara, Y., Saito, T., Masuda, Y., and Nakaya, H. (1995). Anticholinergic effects of class III antiarrhythmic drugs in guinea pig atrial cells. *Circulation*. 91; 2834-2843.
40. Mudd, J. O., and Kass, D. A. (2008). Tackling heart failure in the twenty-first century. *Nature*. 451; 919-928.
41. Nakajima, T., Kurachi, Y., Ito, H., Takikawa, R., and Sugimoto, T. (1988). Anti-cholinergic effects of quinidine, disopyramide, and procainamide in isolated atrial myocytes: Mediation by different molecular mechanisms. *Circulation Research*. 64; 297-303.
42. Ogletree-Hughes, M.L., Stull, L.B., Sweet, W.E., Smedira, N.G., McCarthy, P.M., Moravec, C.S. (2001). Mechanical unloading restores beta-adrenergic responsiveness and reverses receptor downregulation in the failing human heart. *Circulation*. 104; 881-886.
43. Oka, T. and Komuro, I. (2008). Molecular mechanisms underlying the transition of cardiac hypertrophy to heart failure. *Circulation*. Suppl A: A-13-A-16.
44. Olshansky, B., Sabbah, H. N., Hauptamn, P. J., Colucci, W. S. (2008). Parasympathetic nervous system and heart failure: Pathophysiology and potential implications for therapy. *Circulation*. 118:863-871.
45. Peralta, E. G., Ashkenazi, A., Winslow, J. W., and Smith, D. H. (1987). Distinct primary structures, ligand-binding properties and tissue-specific expression of four human muscarinic acetylcholine receptors. *The EMBO Journal*. 6;3923-3929.

46. Perez, C.C.N., Tobar, I.D.B., Jimenez, E., Castaneda, D., Rivero, M.B., Concepcion, J.L., Chiurillo, M.A., and Bonfante-Cabarcas, R. (2006). Kinetic and molecular evidences that human cardiac muscle express non M2 muscarinic receptor subtypes that are able to interact themselves. *Pharmacological Research*. 54; 345-355.
47. Rockman, H. A., Koch, W. J., and Lefkowitz, R. J. (2002). Seven-transmembrane-spanning receptors and heart function. *Nature*. 415;206-212.
48. Rose, E.A., Gelijns, A.C., Moskowitz, A.J., Heitjan, D.F., Stevenson, L.W., Dembitsky, W., Long, J.W., Ascheim, D.D., Tierney, A.R., Levitan, R.G., Watson, J.T., and Meier, P. (2001). Long-term use of a left ventricular assist device for end-stage heart failure. *The New England Journal of Medicine*. 345; 1435-1443.
49. Saladin, K. (2007). *Anatomy and Physiology, The Unity of Form and Function*. Fourth Edition. 564-578.
50. Schmitz, W., Boknik, P., Linck, B., and Muller, F. U. (1996). Adrenergic and muscarinic receptor regulation and therapeutic implications in heart failure. *Molecular and Cellular Biochemistry*. 157; 251-258.
51. Schwartz, P.J., De Ferrari, G.M., Sanzo, A., Landoline, M., Rordorg, R., Raineri, C., Campana, C., Revera, M., Ajmone-Marsan, N., Tavazzi, L, and Otero, A. (2008). Long term vagal stimulation in patients with advanced heart failure First experience in man. *European Journal of Heart Failure*. 884-891.
52. Shi, H., Wang, H., and Wang, Z. (1999). Identification and characterization of multiple subtypes of muscarinic acetylcholine receptors and their physiological functions in canine hearts. *Molecular Pharmacology*. 55; 497-507.
53. Terracciano, C.M., Koban, M.U., Soppa, G.K., et al. (2007). The role of the cardiac Na⁺/Ca²⁺ exchanger in reverse remodeling: relevance for LVAD-recovery. *Annals of the New York Academy of Sciences*. 1099; 349-360.
54. Tracey, K.J. (2002). The inflammatory reflex. *Nature*. 420; 853-859.
55. Triposkiadis, F., Karayannis, G., Giamouzis, G., Skoularigis, J., Louridas, G., and Butler, J. (2009). The sympathetic nervous system in heart failure. *Journal of the American College of Cardiology*. 54:19; 1747-1762.
56. Vatner, D.E., Lee, D.L., Schwarz, K.R., Longabaugh, J.P., Fujii, A.M., Vatner, S.F., and Homcy, C.J. (1988). Impaired cardiac muscarinic receptor function in dogs with heart failure. *Journal of Clinical Investigation*. 81; 1836-1842.

57. Vatner, D.E., Sato, N., Galper, J.B., and Vatner, S.F. (1996). Physiological and biochemical evidence for coordinate increases in muscarinic receptors and Gi during pacing-induced heart failure. *Circulation*. 94; 102-107.
58. Wang, H., Han, H., Zhang, L., Shi, H., Schram, G., Nattel, S., and Wang, Z. (2001). Expression of multiple subtypes of muscarinic receptors and cellular distribution in the human heart. *Molecular Pharmacology*. 59; 1029-1036.
59. Wexler, R., Elton, T., and Pleister, A. (2009). Cardiomyopathy: An overview. *American Family Physician*. 79; 778-784.
60. Wilkinson, M., Giles, A.I., Armour, A., and Cardinal, R. (1996). Ventricular, but not atrial, M2-muscarinic receptors increase in the canine pacing-overdrive model of heart failure. *Canadian Journal of Cardiology*. 11; 71-76.
61. Zhang, Y., Popovic, Z.B., Bibevski, S., Fakhry, I., Sica, D.A., Van Wagoner, D.R., and Mazgalev, T.N. (2009). Chronic vagus nerve stimulation improves autonomic control and attenuates systemic inflammation and heart failure progression in a canine high-rate pacing model. *Circulation*. 120; 692-699.
62. Zhao, Q., Huang, C., Liang, J., Chen, H., Yang, B., Jiang, H., and Li, G. (2008). Effect of vagal stimulation and differential densities of M2 receptor and I_{K,ACh} in canine atria. *International Journal of Cardiology*. 126; 352-358.